on the panel) revealed marked inflammatory reactions with acanthosis and ulceration in epidermis, and marked edema with cellular infiltration including mononuclear cells and neutrophils in the dermis. The skin infiltration of inflammatory cells and epidermal thickness were decreased in rhPIV2/Ag85B treated group (Ag85B ear and Ag85B nasal on the panel). Original magnification × 100. **D.** Plasma IgE levels on day 21. Plasma IgE level was decreased in rhPIV2/Ag85B treated groups (Ag ear and Ag nasal). *P<0.05, **P<0.01.
doi:10.1371/journal.pone.0066614.g003

investigated efficiency of rhPIV2 vaccine vector expressing enhanced green fluorescence protein (EGFP) gene (rhPIV2/EGFP) in infection and expression in vitro and in vivo. Then, we evaluated effectiveness of the vaccination pathways: subcutaneous or intranasal administration of rhPIV2 expressing Ag85B gene (rhPIV2/Ag85B) in a mice AD model induced by repeated hapten challenge.

Materials and Methods

Animals

BALB/c 6-week old male mice were purchased from Japan SLC Co. (Shizuoka, Japan) and used at 7-week. Animal care was performed according to ethical guidelines, and approved by the Institutional Board Committee for Animal Care and Use of Mie University.

Construction of rhPIV2/Ag85B and rhPIV2/EGFP

rhPIV2/Ag85B and rhPIV2/EGFP was constructed according to the method reported previously, except for methods of the supply of T7 and hPIV2 RNA polymerases (NP, P, L). In brief, to generate replication-deficient rhPIV2 vector, two nucleotides change [ATG to TAG (position of 89aa) and AAG to TAG (259aa)] were introduced into the M frame of the plasmid pPIV2, a full-length cDNA copy of hPIV2 anti-genome [19] (Fig. 1A). Consequently, the 6 n length cDNA of Ag85B or EGFP, followed by transcriptional end sequence of NP gene (R2), intergenic sequence (IG), and transcriptional start signal of V/P gene (R1) ([20] was synthesized by PCR using appropriate primers), was inserted into a Not I site of the plasmid DNA encoding the replication-deficient rhPIV2 genome described above. Then, the viruses (rhPIV2/Ag85B and rhPIV2/EGFP) were recovered by co-transfection of each anti-genomic plasmid and plasmids expressing the NP, P, M and L, each cloned in a mammalian gene expression vector (pCAGGS) [21] into BSR7/5 cells expressing T7 RNA polymerase [22]. The cells were harvested, and then co-cultured with fresh Vero cells every 48 hr. Approximately 90% of the cells showed syncytia formation in the 10^{th} co-cultured cells, and its state was maintained in further co-culture. Furthermore, for virus propagation, Cos7 cells were transfected with the plasmid expressing M and co-cultured with above-mentioned 10^{th} cells. The supernatant was centrifuged at 9,000 g for 12 h at 4°C. The virus pellet was suspended in Opti-MEM (Invitrogen, Carisbad, CA, USA). The virus titers were determined by CPE method using Vero cells, and were expressed as 50% tissue culture infectious dose ($TCID_{50}$).

In vitro and in vivo Infection of rhPIV2 Vector Expressing EGFP

HaCat cells (Cell Line Service, Eppelheim, Germany) were cultured in Dulbecco's MEM supplemented with 5% (v/v) FBS, 2.0 mM L-glutamine, 100 U/ml penicillin, and 100 mg/ml streptomycin. HaCat cells were seeded one day before the transduction at 1×10^6 cells/ml (1 ml/well) in 6-well culture plates (Costar, NY, USA). The cells were incubated for 8 hours at 37°C in a 5% CO_2 atmosphere. The next day, the media was removed and 1 ml of the rhPIV2/EGFP viruses were added to the cells to be adjusted to 1×10^6 $TCID_{50}$. Two hours after infection, the media was removed and fresh culture media was supplemented to the cells. After 3 days culture, each well was observed by fluorescence microscopy.

At the next step, 20 μl of concentrated rhPIV2/EGFP (5×10^6 $TCID_{50}$) were administered into the cavity of the nose of the mice. Four days after infection, the respiratory tract and lung were sampled, embedded in Tissue-Tek OCT compound (Miles, Elkhart, USA), frozen in liquid nitrogen, and cut into 7 μm-thick sections. Sections were examined and recorded by fluorescence microscopy.

Sensitization and Challenge Schedule

Repeated hapten sensitization and challenge system was introduced in this experiment. OX (Sigma, St. Louis, MO) was dissolved in acetone/olive oil (1:1). As shown in Fig. 1B, mice were initially sensitized by pasting 20 μl of 0.5% OX solution to their right ear 7 days prior to the first challenge (day -7) and then 20 μl of 0.5% OX solution was repeatedly applied on the right ear 3 times per week from day 0 until day 21. Repeated application of OX causes delayed type hypersensitivity followed by immediate-type and late phase reaction. For vaccination, mice were infected intranasally under general anesthesia with 5×10^6 $TCID_{50}$ of the virus in a 20 μl inoculum or phosphate-buffered saline (PBS) on day 4. On day 16, mice were vaccinated again with PBS, rhPIV2/Ag85B or control rhPIV2 vector intranasally or subcutaneously to the pinna skin (Fig. 1B,C). Ear swelling was measured with thickness gauge calipers before and 6 hours after last OX challenge on day 21. Blood and pinna skins were also sampled.

Histopathological Study

The ear skins were sampled at six hours after last OX challenge on day 21. Samples were fixed in 10% neutral buffered formaldehyde and embedded in paraffin. Histological sections were of 6 mm thickness and stained with hematoxylin & eosin (H&E).

Analysis of Cytokine mRNA Expression in Mouse Ear

The mRNA was extracted from the mouse ear using Isogen (Nippon Gene, Tokyo, Japan) according to the manufacturer's instructions: One ml of homogenate was mixed with 200 μl of chloroform, and then centrifuged. The aqueous phase was separated and mixed with 0.5 ml of 2-propanol (Nacalai Tesque, Kyoto, Japan) to precipitate RNA. After centrifuging, the precipitate was washed with 70% ethanol (Nacalai Tesque) and the RNA was suspended in 40 μl of RNase-free water. The concentration of RNA was measured at 260 nm absorbent, and the quality was confirmed by electrophoresis. cDNA was synthesized from 2 μg of mRNA using an archive kit (Applied Biosystems, Foster City, CA, USA) according to the manufacturer's protocol. Real time quantitative reverse transcription-polymerase chain reaction (RT-PCR) was performed to measure transcriptional activity in skin lesions. A 25 μl reaction mixture containing 1 μg of cDNA, 900 nM of each primer, and 250 nM of TaqMan probe was mixed with 12.5 μl of TaqMan Master Mix (AB). Quantitative RT-PCR for cytokine transcripts was performed using prequalified primers and probes for IL-2, IL-4, IL-10, IL-17A, MIP2, TNF-α, TGF-β, IFN-γ and GAPDH (AB). The

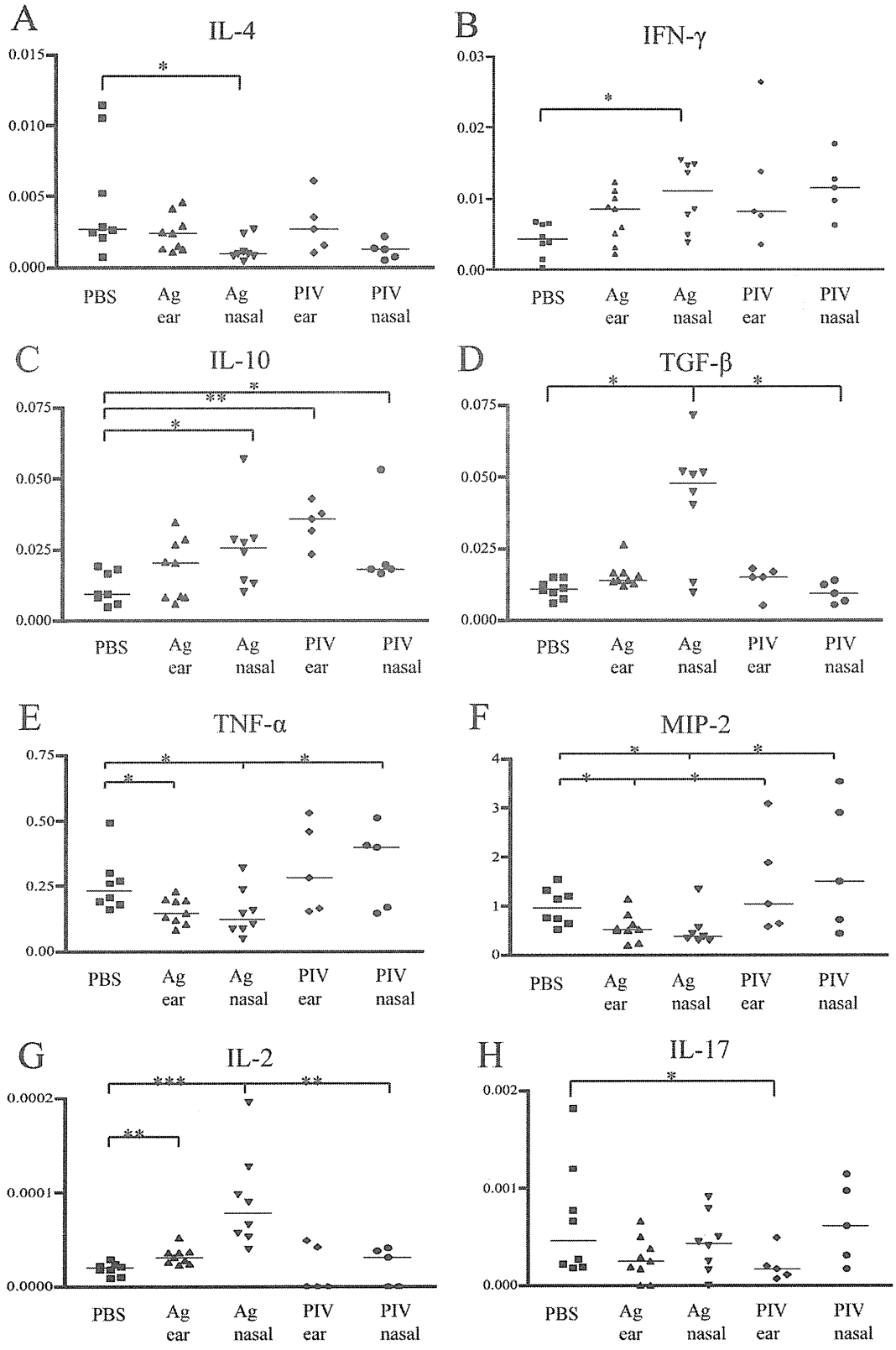
A
IL-4
0.015
0.010
0.005
0.000
*
PBS
Ag ear
Ag nasal
PIV ear
PIV nasal
B
IFN-γ
0.03
0.02
0.01
0.00
*
PBS
Ag ear
Ag nasal
PIV ear
PIV nasal
C
IL-10
0.075
0.050
0.025
0.000
*
**
*
PBS
Ag ear
Ag nasal
PIV ear
PIV nasal
D
TGF-β
0.075
0.050
0.025
0.000
*
*
PBS
Ag ear
Ag nasal
PIV ear
PIV nasal
E
TNF-α
0.75
0.50
0.25
0.00
*
*
*
PBS
Ag ear
Ag nasal
PIV ear
PIV nasal
F
MIP-2
4
3
2
1
0
*
*
*
PBS
Ag ear
Ag nasal
PIV ear
PIV nasal
G
IL-2
0.0002
0.0001
0.0000
***
**
**
PBS
Ag ear
Ag nasal
PIV ear
PIV nasal
H
IL-17
0.002
0.001
0.000
*
PBS
Ag ear
Ag nasal
PIV ear
PIV nasal

Figure 4. Changes in cytokines mRNA expression levels in the ears of AD mice by vaccination of rhPIV2/Ag85B. Cytokines: IL-4 (panel A), IFN-γ (panel B), IL-10 (panel C), TGF-β (panel D), TNF-α (panel E), MIP2-α (panel F), IL-2 (panel G), IL-17 (panel H), mRNA expression in the ear lesions measured with Quantitative RT-PCR. Expressions of IL-4, TNF-α and MIP2-α mRNA were significantly decreased in the ear skin treated with intra-nasally rhPIV2/Ag85B treated group compared to those of control groups. Meanwhile, the expression levels of mRNA of IFN-γ, IL-10, TGF-β and IL-2 were significantly elevated in rhPIV2/Ag85B intra-nasally treated group compared to those of control groups. *P<0.05, **P<0.01, ***P<0.001.
doi:10.1371/journal.pone.0066614.g004

ΔCt method was used to standardize the transcripts to GAPDH, and the ratio to that of control mice was calculated.

Immunohistochemistry

The ear skins sampled on day 21 were snap-frozen, and the frozen sections prepared at 7 μm thickness were subjected to a blocking procedure with 5% normal goat serum (Vector Laboratories, Burlingame, CA). Sections were then incubated with FITC-conjugated rat anti-mouse CD4 antibody (Beckman Coulter) and PE conjugated anti-mouse FoxP3 antibody (BioLegend), and examined under Fluoview FV1000 laser scanning confocal microscopy (Olympus, Tokyo, Japan). Skin infiltrating $CD4^+$ T cells and $FoxP3^+CD4^+$ T cells were counted at x100 field, and the numbers in 10 randomly chosen fields of five samples were evaluated.

Measurement of Serum IgE

Serum IgE level was determined by a sandwich enzyme-linked immunosorbent assay (Yamasa, Tokyo, Japan) according to the manufacturer's instructions. Optical density of each well was determined by using a microplate reader (Multiscan JX, Thermo Electron, Yokohama, Japan).

Statistical Analysis

Statistical analysis was performed using Mann-Whitney U-test. $P<0.05$ was considered as significant.

Results

rhPIV2/EGFP Infection in vitro and in vivo

To investigate expression levels of the inserted gene in rhPIV2 in vitro, HaCat cells were infected with rhPIV2/EGFP at an MOI of 0.5 and were examined directly using a fluorescence microscopy. The EGFP from rhPIV2/EGFP was highly expressed in HaCat cells, and remarkable fluorescence extended to nearly all the cells in spite of low MOI (Fig. 2A). Then, to evaluate the gene expression in vivo, mice were intra-nasally inoculated with rhPIV2/EGFP (5×10^6 $TCID_{50}$), and the intense EGFP expression was revealed in the lung epithelium of the mice (Fig. 2B).

Cutaneous Manifestations

To evaluate the clinically relevant therapies, mice were treated following the strategy shown in Fig. 1B. Ear lobes of the rhPIV2 (vector alone) or PBS-treated mice developed severe edematous erythema with exudation and erosion at 6 hours after OX challenge on day 21. However, rhPIV2/Ag85B-treatment reduced dermatitis in both of the intra-nasal and subcutaneous application groups (Fig. 3A). Ear swelling was dramatically suppressed in both of the rhPIV2/Ag85B-treated mice compared to PBS or rhPIV2 treated mice (Fig. 3B).

Histopathological Findings

PBS or rhPIV2-treated mice showed marked inflammatory reactions with acanthosis and ulceration in epidermis, and marked edema with cellular infiltration including mononuclear cells and neutrophils in the dermis. Both of the intra-nasal and subcutaneous rhPIV2/Ag85B application successfully reduced inflammatory cell infiltration and epidermal thickness (Fig. 3C).

Serum IgE Levels

High levels of IgE were detected in sera from PBS or rhPIV2-treated mice. On the other hand, the IgE levels in the sera from Ag85B-treated mice by two ways were suppressed significantly (Fig. 3D).

Cytokines mRNA Expression in the Ear Skins

Expression of IL-4 mRNA was significantly decreased in the ear skin of intra-nasally rhPIV2/Ag85B treatment group compared to that of PBS treated mice (Fig. 4A). In clear contrast, IFN-γ mRNA expression was significantly increased in rhPIV2/Ag85B intra-nasally treated group (Fig. 4B). As expected, IL-10 levels were significantly increased in intra-nasally treated with rhPIV2/Ag85B and rhPIV2-vector groups (Fig. 4C). Surprisingly, TGF-β expression is remarkably elevated in the intra-nasal rhPIV2/Ag85B group (Fig. 4D). mRNA expressions of TNF-α and MIP-2 were significantly decreased in both of intra-nasally and subcutaneously rhPIV2/Ag85B treated groups compared with PBS or vector treated group (Fig. 4E, F). The expression of IL-2 mRNA was also significantly elevated in both of the rhPIV2/Ag85B intra-nasally and subcutaneously treated groups (Fig. 4G). No obvious suppression in IL-17 mRNA expression was detected in rhPIV2/Ag85B group (Fig. 4H).

Immunostaining for Tregs in the Inflamed Ear Skin Lesions

As shown in Fig. 5A, $CD4^+$ T cells are displayed with green fluorescence, and $Foxp3^+$ T cells are with red. Merged yellow color means $Foxp3^+CD4^+$ T cells. The skin infiltrating $CD4^+$ T cells are significantly decreased in Ag nasal group and Ag ear group compared to that of PBS-treated group. Although it does not reach the significance, the $CD4^+$ T cells number is less in Ag nasal group compared to Ag ear group (Fig. 5B). The $Foxp3^+CD4^+$ T cells are significantly increased in both of Ag nasal and Ag ear groups (Fig. 5C).

Discussion

Immune system is finely controlled on the balance of four main subsets of Th1, Th2, Th17, and Treg [5] cells. AD, especially in its acute phase, is a disease that Th2 cells are dominantly involved in the pathogenesis. In fact PBMCs from patients with AD have increased production of IL-4, IL-5, and IL-13 with limited capacity in production of IFN-γ [23–25]. Repeated elicitation of OX on mice ear shifts the cutaneous Th1 cytokine milieu to Th2, which represents the characteristic immunological features of AD. Immunotherapy for AD has some different options to correct the imbalance of the shifted cytokine profile. In the present study, we investigated effects of vaccination using replication-deficient rhPIV2 vector expressing Ag85B gene to mouse AD model. BCG is known as a strong Th1 response modifier; however, it has a risk for granuloma formation. To avoid granuloma formation, non-wax protein antigen is required. Ag85B is a conserved protein in mycobacterial species and can elicit a strong Th1-type immune

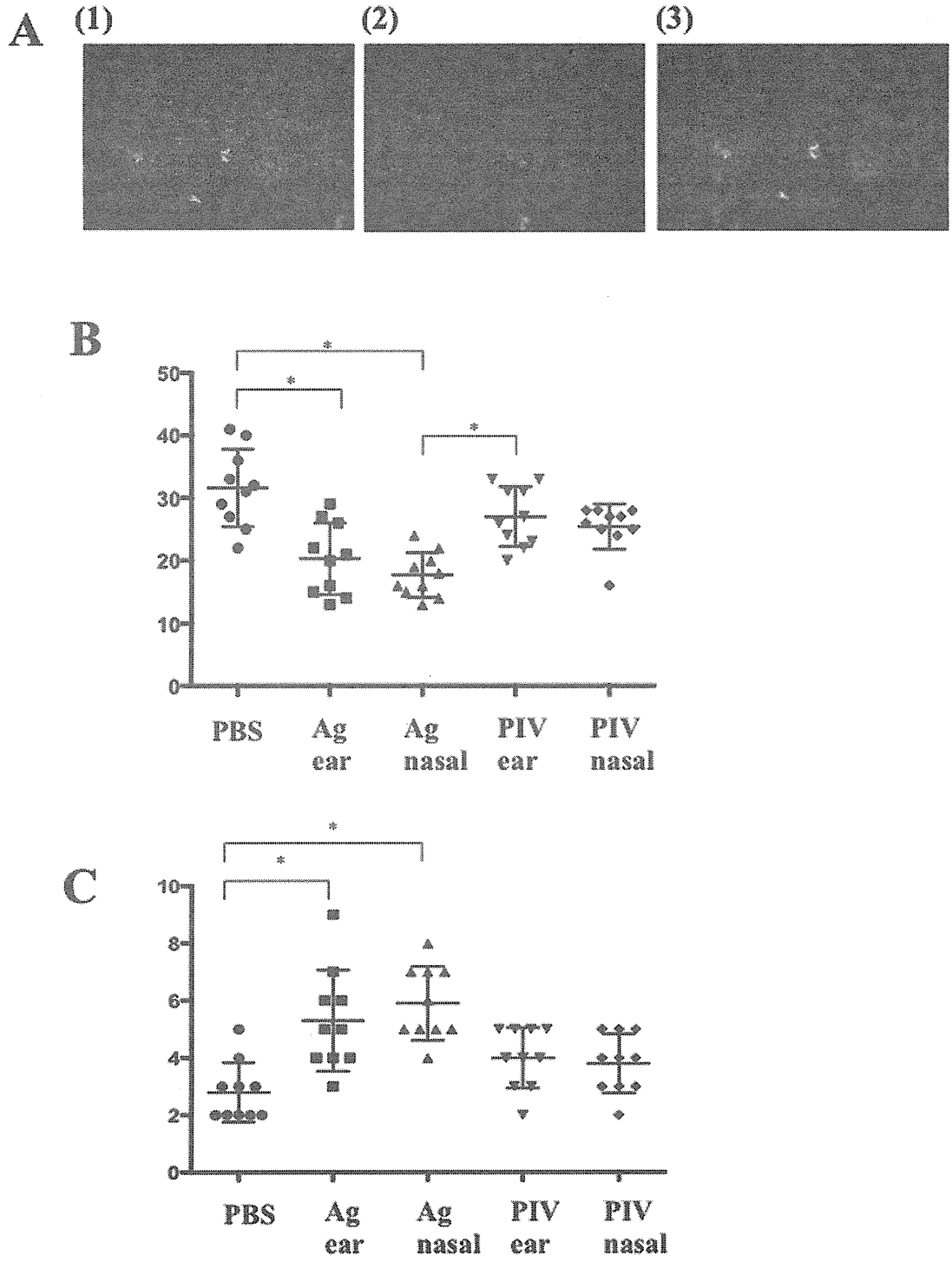

Figure 5. Immunostaining for Tregs in the inflamed ear skin lesions. A. $CD4^+$ T cells are displayed with green fluorescence (1), and $Foxp3^+$ T cells are with red (2). Merged yellow color means $Foxp3^+CD4^+$ T cells (3) (x100). **B.** The number of skin infiltrating $CD4^+$ T cells is less in Ag nasal group and Ag ear group compared to that of PBS-treated group. Although it does not reach statistical significance, $CD4^+$ T cell number is less in Ag nasal group compared to that of Ag ear group. **C.** The number of $Foxp3^+CD4^+$ T cells in the inflamed ear skin is significantly increased in both of the intra-nasal and ear-subcutaneous rhPIV2/Ag85B application groups.
doi:10.1371/journal.pone.0066614.g005

response [8]. Therefore, Ag85B has been used as immune-modulator to control acute AD lesions or asthma. Ag85B DNA vaccine suppressed airway inflammation in a murine model of asthma [26]. Furthermore, resent studies suggested that Ag85B vaccination promotes Th1-type immune responses as well as Treg responses. Administration of Ag85B showed therapeutic effects to Th2-type cytokine mediated acute phase AD models by inducing regulatory T cells [10].

Selection of the vector and its application pathway has importance in successful DNA vaccination therapy. We selected hPIV2 as a potential vector for Ag85B vaccination. hPIVs are human respiratory pathogens, and the most distinctive clinical feature of infection of hPIVs is croup (i.e., laryngotracheobronchitis or swelling around the vocal chords and other parts of the upper and middle airway). Among hPIVs, hPIV1 and hPIV3 are the major cause of croup in children, whereas hPIV2 is rarely identified as a clinical pathogen. Therefore, hPIV2 has been suspected as less virulent and cytotoxic virus. hPIV2 enters the cell by cell fusion at the plasma membrane, and replicates exclusively in the cytoplasm, and buds at the plasma membrane. Therefore, hPIV2 has no risk for integration in the host genome, not like retrovirus. In addition, since hPIV2 has a non-segmented and negative-stranded RNA genome, there is no antigenic shift among RNA segments, not like influenza viruses. Using technology of advanced reverse genetics [20], we constituted replication-deficient hPIV2 vector with additional advantage as a highly safe virus vector. To confirm the target and effective infection of rhPIV2 vector, we inoculated rhPIV2/EGFP to HaCat cells. HaCat cells successfully expressed EGFP up to 7 days post-infection (pi). Also, BALB/c mice intranasally single-administrated with rhPIV2/EGFP showed intense EGFP expression in the airway epithelial cells. These results strongly support activities of long-term high-level expression of the exogenous gene and efficiency of rhPIV2 in vivo.

In the present study, AD symptoms including ear swelling at late phase reaction were significantly suppressed in rhPIV2/Ag85B treated groups in both of intra-nasal and subcutaneous administration. Inflammatory cell infiltration including mast cells and eosinophils in the lesional skin was also suppressed. In the cytokine profile, mRNA expression of IFN-γ and IL-2 in the ear skins was significantly increased. Interestingly, IL-4 mRNA was significantly reduced in intranasal rhPIV2/Ag85B treated groups. In IL-4 suppression and IFN-γ induction, intra-nasal application showed stronger effects compared with subcutaneous application. hPIV2 is a virus infectious to the respiratory tract mucosa, and therefore more effective capture of rhPIV2/Ag85B by respiratory epithelium compared with that of skin resident cells is reasonable. In addition, the skin derived anti-infectious molecule, horny layer proteases and epithelial skin barrier might decrease efficiency of rhPIV2.

Treg induction in the effects of rhPIV2/Ag85B therapy has importance. Present study unveiled augmentation of TGF-β and IL-10 expression by intranasal rhPIV2/Ag85B. TGF-β and IL-10 have been described as critical regulatory cytokines produced by Treg. In fact in the current experiment, the numbers of skin infiltrating $CD4^+$ T cells are decreased in the nasal application and ear skin application groups accompanied with increased $FoxP3^+$ Treg population. A heat-killed Mycobacterium vaccae (*M. vaccae*) gives rise to allergen specific regulatory T cells that produce IL-10 and TGF-β, which confer the protection against airway inflammation [27]. Recently TGF-β was proved to suppress GATA-3 function through Sox4 signal, and TGF-β controls Th2 cell-mediated inflammation [28]. In addition, it is crucial that PIV2 itself has some effects in induction of Treg without obvious effects in clinical manifestation and Th1/Th2 balance.

In conclusion, the respiratory tract epithelium captured rhPIV2 effectively without remarkable cytotoxic effects. The treatment with rhPIV2/Ag85B especially by trans-nasal mucosa approach ameliorates OX-induced AD model by altering Th2/Th1 cytokine balance with induction of regulatory cytokines induction. Thus, nasal rhPIV2/Ag85B vaccination is a novel, less invasive and useful therapeutic approach for AD and related allergic disorder.

Acknowledgments

We thank Dr. K.K. Conzelmann for BSRT7/5 cells.

Author Contributions

Conceived and designed the experiments: H. Kitagawa M. Kawano. Performed the experiments: H. Kitagawa M. Kawano HI MY TS AN KN. Analyzed the data: H. Kitagawa M. Kawano. Contributed reagents/materials/analysis tools: M. Kakeda KT H. Komada MT YY. Wrote the paper: H. Kitagawa M. Kawano KY TN HM.

References

1. Grewe M, Bruijnzeel-Koomen CA, Schopf E, Thepen T, Langeveld-Wildschut AG, et al. (1998) A role for Th1 and Th2 cells in the immunopathogenesis of atopic dermatitis. Immunol Today 19: 359–361.
2. Kondo H, Ichikawa Y, Imokawa G (1998) Percutaneous sensitization with allergens through barrier-disrupted skin elicits a Th2-dominant cytokine response. Eur J Immunol 28: 769–779.
3. Ou LS, Goleva E, Hall C, Leung DY (2004) T regulatory cells in atopic dermatitis and subversion of their activity by superantigens. J Allergy Clin Immunol 113: 756–763.
4. Ito Y, Adachi Y, Makino T, Higashiyama H, Fuchizawa T, et al. (2009) Expansion of FOXP3-positive CD4+CD25+ T cells associated with disease activity in atopic dermatitis. Ann Allergy Asthma Immunol 103: 160–165.
5. Yamanaka K, Mizutani H (2011) The role of cytokines/chemokines in the pathogenesis of atopic dermatitis. Current problems in dermatology 41: 80–92.
6. Kitagaki H, Ono N, Hayakawa K, Kitazawa T, Watanabe K, et al. (1997) Repeated elicitation of contact hypersensitivity induces a shift in cutaneous cytokine milieu from a T helper cell type 1 to a T helper cell type 2 profile. J Immunol 159: 2484–2491.
7. Nagai S, Wiker HG, Harboe M, Kinomoto M (1991) Isolation and partial characterization of major protein antigens in the culture fluid of Mycobacterium tuberculosis. Infect Immun 59: 372–382.
8. Takatsu K, Kariyone A (2003) The immunogenic peptide for Th1 development. Int Immunopharmacol 3: 783–800.
9. Russo DM, Kozlova N, Lakey DL, Kernodle D (2000) Naive human T cells develop into Th1 effectors after stimulation with Mycobacterium tuberculosis-infected macrophages or recombinant Ag85 proteins. Infect Immun 68: 6826–6832.
10. Mori H, Yamanaka K, Matsuo K, Kurokawa I, Yasutomi Y, et al. (2009) Administration of Ag85B showed therapeutic effects to Th2-type cytokine-mediated acute phase atopic dermatitis by inducing regulatory T cells. Arch Dermatol Res 301: 151–157.
11. Kakeda M, Yamanaka K, Kitagawa H, Tsuda K, Akeda T, et al. Heat-killed bacillus Calmette-Guerin and Mycobacterium kansasii antigen 85B combined vaccination ameliorates dermatitis in a mouse model of atopic dermatitis by inducing regulatory T cells. Br J Dermatol 166: 953–963.
12. Kawano M, Bando H, Ohgimoto S, Okamoto K, Kondo K, et al. (1990) Complete nucleotide sequence of the matrix gene of human parainfluenza type 2 virus and expression of the M protein in bacteria. Virology 179: 857–861.
13. Kawano M, Bando H, Ohgimoto S, Kondo K, Tsurudome M, et al. (1990) Sequence of the fusion protein gene of human parainfluenza type 2 virus and its 3′ intergenic region: lack of small hydrophobic (SH) gene. Virology 178: 289–292.
14. Ohgimoto S, Bando H, Kawano M, Okamoto K, Kondo K, et al. (1990) Sequence analysis of P gene of human parainfluenza type 2 virus: P and cysteine-rich proteins are translated by two mRNAs that differ by two nontemplated G residues. Virology 177: 116–123.
15. Lamb RA, Kolakofsky D (2001) Paramyxoviridae: the viruses and their replicatio. In: Knipe DM, Howley PM, editors. In Fields Virology. Fourth ed. Philadelphia: Lippincott Williams & Wilkins. 1305–1340.

16. Schnell MJ, Mebatsion T, Conzelmann KK (1994) Infectious rabies viruses from cloned cDNA. EMBO J 13: 4195–4203.
17. Bukreyev A, Lamirande EW, Buchholz UJ, Vogel LN, Elkins WR, et al. (2004) Mucosal immunisation of African green monkeys (Cercopithecus aethiops) with an attenuated parainfluenza virus expressing the SARS coronavirus spike protein for the prevention of SARS. Lancet 363: 2122–2127.
18. Tompkins SM, Lin Y, Leser GP, Kramer KA, Haas DL, et al. (2007) Recombinant parainfluenza virus 5 (PIV5) expressing the influenza A virus hemagglutinin provides immunity in mice to influenza A virus challenge. Virology 362: 139–150.
19. Kawano M, Kaito M, Kozuka Y, Komada H, Noda N, et al. (2001) Recovery of infectious human parainfluenza type 2 virus from cDNA clones and properties of the defective virus without V-specific cysteine-rich domain. Virology 284: 99–112.
20. Kawano M, Okamoto K, Bando H, Kondo K, Tsurudome M, et al. (1991) Characterizations of the human parainfluenza type 2 virus gene encoding the L protein and the intergenic sequences. Nucleic Acids Res 19: 2739–2746.
21. Niwa H, Yamamura K, Miyazaki J (1991) Efficient selection for high-expression transfectants with a novel eukaryotic vector. Gene 108: 193–199.
22. Buchholz UJ, Finke S, Conzelmann KK (1999) Generation of bovine respiratory syncytial virus (BRSV) from cDNA: BRSV NS2 is not essential for virus replication in tissue culture, and the human RSV leader region acts as a functional BRSV genome promoter. J Virol 73: 251–259.
23. Jung T, Lack G, Schauer U, Uberuck W, Renz H, et al. (1995) Decreased frequency of interferon-gamma- and interleukin-2-producing cells in patients with atopic diseases measured at the single cell level. J Allergy Clin Immunol 96: 515–527.
24. Matsuyama T, Urano K, Ohkido M, Ozawa H, Ohta A, et al. (1999) The quantitative and qualitative defect of CD4+ CD45RO+ memory-type T cells are involved in the abnormality of TH1 immunity in atopic dermatitis patients. Clin Exp Allergy 29: 687–694.
25. Reinhold U, Wehrmann W, Kukel S, Kreysel HW (1990) Evidence that defective interferon-gamma production in atopic dermatitis patients is due to intrinsic abnormalities. Clin Exp Immunol 79: 374–379.
26. Wu J, Xu J, Cai C, Gao X, Li L, et al. (2009) Ag85B DNA vaccine suppresses airway inflammation in a murine model of asthma. Respir Res 10: 51.
27. Zuany-Amorim C, Sawicka E, Manlius C, Le Moine A, Brunet LR, et al. (2002) Suppression of airway eosinophilia by killed Mycobacterium vaccae-induced allergen-specific regulatory T-cells. Nat Med 8: 625–629.
28. Kuwahara M, Yamashita M, Shinoda K, Tofukuji S, Onodera A, et al. (2012) The transcription factor Sox4 is a downstream target of signaling by the cytokine TGF-beta and suppresses T(H)2 differentiation. Nat Immunol 13: 778–786.

Differentiation 85 (2013) 131–139

Contents lists available at SciVerse ScienceDirect

Differentiation

journal homepage: www.elsevier.com/locate/diff

Cynomolgus monkey induced pluripotent stem cells established by using exogenous genes derived from the same monkey species

Nobuhiro Shimozawa [a,*], Ryoichi Ono [b], Manami Shimada [c], Hiroaki Shibata [a], Ichiro Takahashi [d], Hiroyasu Inada [e], Tatsuyuki Takada [c], Tetsuya Nosaka [b], Yasuhiro Yasutomi [a,f]

[a] Tsukuba Primate Research Center (TPRC), National Institute of Biomedical Innovation (NIBIO), 1-1 Hachimandai, Tsukuba, Ibaraki 305-0843, Japan
[b] Department of Microbiology and Molecular Genetics, Mie University Graduate School of Medicine, 2-174 Edobashi, Tsu, Mie 514-8507, Japan
[c] Laboratory of Cell Engineering, Department of Pharmaceutical Sciences, Ritsumeikan University, 1-1-1 Noji-higashi, Kusatsu, Shiga 525-8577, Japan
[d] Laboratory of Rare Disease Biospecimen, NIBIO, 7-6-8 Saito-Asagi, Ibaragi, Osaka 567-0085, Japan
[e] Department of Pathology, Faculty of Pharmaceutical Science, Suzuka University of Medical Science, 3500-3 Minamitamagaki-cho, Suzuka, Mie 513-8670, Japan
[f] Division of Immunoregulation, Department of Molecular and Experimental Medicine, Mie University Graduate School of Medicine, 2-174 Edobashi, Tsu, Mie 514-8507, Japan

ARTICLE INFO

Article history:
Received 28 May 2012
Received in revised form
29 January 2013
Accepted 23 February 2013

Keywords:
Induced pluripotent stem cells
Cynomolgus monkey
Cynomolgus monkey genes
Non-human primate
Medical research

ABSTRACT

Induced pluripotent stem (iPS) cells established by introduction of the transgenes POU5F1 (also known as Oct3/4), SOX2, KLF4 and c-MYC have competence similar to embryonic stem (ES) cells. iPS cells generated from cynomolgus monkey somatic cells by using genes taken from the same species would be a particularly important resource, since various biomedical investigations, including studies on the safety and efficacy of drugs, medical technology development, and research resource development, have been performed using cynomolgus monkeys. In addition, the use of xenogeneic genes would cause complicating matters such as immune responses when they are expressed. In this study, therefore, we established iPS cells by infecting cells from the fetal liver and newborn skin with amphotropic retroviral vectors containing cDNAs for the cynomolgus monkey genes of POU5F1, SOX2, KLF4 and c-MYC. Flat colonies consisting of cells with large nuclei, similar to those in other primate ES cell lines, appeared and were stably maintained. These cell lines had normal chromosome numbers, expressed pluripotency markers and formed teratomas. We thus generated cynomolgus monkey iPS cell lines without the introduction of ecotropic retroviral receptors or other additional transgenes by using the four allogeneic transgenes. This may enable detailed analysis of the mechanisms underlying the reprogramming. In conclusion, we showed that iPS cells could be derived from cynomolgus monkey somatic cells. To the best of our knowledge, this is the first report on iPS cell lines established from cynomolgus monkey somatic cells by using genes from the same species.

1. Introduction

Pluripotent stem cells that have competence similar to embryonic stem (ES) cells have been artificially generated from mouse somatic cells *in vitro* (Takahashi and Yamanaka, 2006). Establishment of this cell population, named induced pluripotent stem (iPS) cells, was achieved by introduction of the exogenous transgenes POU5F1 (also known as Oct3/4), SOX2, KLF4 and c-MYC using retroviral vectors. The iPS cell lines showed the characteristic morphologies and protein and gene expressions, as well as the karyotype stability and differentiation ability, of ES cells. It was also confirmed that mouse iPS cells differentiated into functional germ cells in the chimera gonads (Okita et al., 2007). Furthermore, iPS cells were successfully established from human somatic cells (Takahashi et al., 2007).

Cynomolgus monkeys (*Macaca fascicularis*) are one of the most important species of non-human primates, and are essential to biomedical research due to their close relationship to humans. In addition, cynomolgus monkeys are annual breeders, and in this respect are more similar to humans than rhesus monkeys, which are seasonal breeders. In non-human primates, the establishment of ES cell lines has been reported in the rhesus monkey (*Macaca mulatta*) (Thomson et al. 1995), the common marmoset (*Callithrix jacchus*) (Thomson et al. 1996), the cynomolgus monkey (Suemori et al., 2001) and the African green monkey (*Cercopithecus aethiops*) (Shimozawa et al., 2010). Before ES cells can be used for clinical

* Corresponding author. Tel.: +81 29 837 2121; fax: +81 29 837 0218.
E-mail address: shimo@nibio.go.jp (N. Shimozawa).

0301-4681/$ - see front matter © 2013 International Society of Differentiation. Published by Elsevier B.V. All rights reserved.
Join the International Society for Differentiation (www.isdifferentiation.org)
http://dx.doi.org/10.1016/j.diff.2013.02.004

applications in humans, research using non-human primates, especially cynomolgus monkeys, will be needed to examine their safety and efficacy.

Among non-human primates, iPS cells have been established in rhesus monkeys (Liu et al., 2008) and common marmosets (Tomioka et al., 2010) and cynomolgus monkeys (Okahara-Narita et al., 2012). Research into regenerative medicine using rhesus monkeys, common marmosets and cynomolgus monkeys is particularly active, and the differentiation of ES cells into various somatic cells is also being widely studied. Similar studies have also been performed on iPS cells. However, some abnormal characteristics of iPS cells have been reported (Kim et al., 2010; Lister et al., 2011; Nishino et al., 2011), and there is uncertainty with regard to their safety and efficacy. Therefore, the ideal induction methods for achieving fully reprogrammed pluripotent stem cells are currently under investigation (Maekawa et al., 2011).

The Tsukuba Primate Research Center (TPRC) in Japan has a specific pathogen-free (SPF) colony of cynomolgus monkeys that have been maintained by indoor breeding as a closed colony with an absence of microorganism infections (Honjo, 1985; Yasutomi, 2010). Using such monkeys, the safety and efficacy of drugs, medical technology development and research resource development can be researched. Because cynomolgus monkeys are used for various types of medical research, unexpected disadvantageous effects due to the use of genes from different species need to be excluded. Therefore, to establish iPS cells, we introduced four genes (POU5F1, SOX2, KLF4 and c-MYC) cloned from cynomolgus monkeys using the amphotropic retroviral vectors produced from Plat-A cells into the somatic cells of the cynomolgus monkeys. To the best of our knowledge, this is the first report on the establishment of cynomolgus monkey iPS cell lines using genes from the monkeys themselves.

2. Materials and methods

2.1. Animals

The cynomolgus monkeys (*Macaca fascicularis*) used in this study were bred and maintained in an air-conditioned room at the TPRC with controlled illumination (12 h light/12 h dark), temperature (25±2 °C), humidity (60±5%), and ventilation (10 cycles/h), and were given 70 g of commercial food (Type AS; Oriental Yeast Co., Ltd., Tokyo, Japan) and 100 g of apples daily, and unlimited access to tap water (Tsuchida et al., 2008). Every morning their health status (*e.g.*, viability, appetite, fur-coat appearance) was monitored. The maintenance of animals was conducted according to the rules for animal care of the TPRC at the National Institutes of Biomedical Innovation (NIBIO) for the care, use, and biohazard countermeasures of laboratory animals. All animal experiments were conducted in accordance with the guidelines for animal experiments of the NIBIO.

2.2. Cell culture

The newborn skin and fetal liver tissues utilized in this study were collected from the fetus and newborn delivered by Cesarean section for other studies. The tissues were thoroughly minced with scissors. The minced tissue pieces were cultured in Dulbecco's modified Eagle's medium (DMEM; Wako Pure Chemical Industries, Ltd., Osaka, Japan) with 10% fetal bovine serum (FBS; Wako Pure Chemical Industries) and 1% penicillin–streptomycin solution (Sigma, St. Louis, MO, USA). Primary cultures grown to confluence were digested with trypsin–EDTA solution (Sigma) and subcultured. Until culturing for the generation of iPS cells, the cells were kept in a Cell Banker (Nippon Zenyaku Kogyo Co., Ltd., Fukushima, Japan) in liquid nitrogen. Plat-A cells were maintained in DMEM with 10% FBS, 1% penicillin–streptomycin solution, 1 μg/mL puromycin (Sigma) and 10 μg/mL blasticidin S (Sigma). For 24 h before transfection, Plat-A cells were cultured in DMEM with 10% FBS and 1% penicillin–streptomycin solution. Cynomolgus monkey iPS cells were cultured on a mitomycin C-treated mouse embryonic fibroblast (MEF) cell monolayer derived from ICR mice (Charles River Japan, Kanagawa, Japan) on gelatin-coated 10 cm dishes in ES cell culture medium (ESM) consisting of DMEM/F12 (1:1) (Sigma) supplemented with 20% knockout serum replacement (KSR; Invitrogen), 1% GlutaMax (Invitrogen), 0.1 mM β-mercaptethanol (Sigma), 1% non-essential amino acids (Invitrogen), 10 ng/mL human recombinant leukemia inhibitory factor (hLIF; Millipore, Billerica, MA), 4 ng/mL human recombinant basic fibroblast growth factor (hbFGF; Wako Pure Chemical Industries) and 1% penicillin-streptomycin solution. For passaging, iPS cell colonies were treated with 0.1% collagenase (Wako Pure Chemical Industries) in DMEM and divided into small clusters with pipetting, then subcultured onto a new MEF layer.

2.3. Generation of iPS cells

We used KLF4, SOX2, POU5F1 and c-MYC genes from cynomolgus monkeys to establish the iPS cell lines. KLF4 and SOX2 were obtained from the JCRB Gene Bank (http://genebank.nibio.go.jp/). POU5F1 was derived from the cynomolgus monkey ES cell line, CMK6 (AGC Techno Glass Co., Ltd., Chiba, Japan). c-MYC was isolated from cynomolgus monkey skin fibroblast cells activated by bFGF.

Cynomolgus monkey iPS cells were generated as described by Takahashi and Yamanaka (2006) and Takahashi et al. (2007). Briefly, for retrovirus production, pMXs (Kitamura et al., 2003) containing cDNA of cynomolgus monkey POU5F1, SOX2, KLF4 and c-MYC, respectively, were transfected into Plat-A cells (Kitamura et al., 2003) after 24 h of culture using FUGENE6 Transfection Reagent (Roche, Basel, Switzerland). For confirmation of infection to the somatic cells, pMX containing cDNA of GFP was also prepared. After 24 h, the medium was exchanged for 2 mL of fresh medium. Cynomolgus monkey somatic cells from skin and liver were seeded at 1.5–5 × 10^5 cells in 10 cm dishes (BD Falcon, Franklin Lakes, NJ, USA). The next day, the supernatants with viruses produced from Plat-A cells were filtered by a cellulose acetate filter, respectively, and mixed. The somatic cells from skin and liver were infected with 2 mL of the virus-supernatants containing 4 μg/mL polybrene (Sigma) per 6 cm dish, respectively. After 24 h, the supernatants were exchanged with fresh medium. Seven days after infection, the cynomolgus monkey cells were recovered by trypsinization and seeded onto a mitomycin C-treated MEF cell monolayer on gelatin-coated 10 cm dishes in DMEM with 10% FBS and 1% penicillin–streptomycin solution. The next day, the medium was exchanged for ESM. The ES cell-like colonies were divided into small clusters with pipetting and passaged onto new feeder layers.

2.4. In vivo and in vitro differentiation

For pluripotency analysis, teratomas and embryoid bodies (EBs) were derived from iPS cells. Teratoma formation was accomplished as follows. The iPS cells suspended in ESM without β-mercaptethanol, hLIF and hbFGF were injected into the hind leg muscle of immunodeficient mice (NOD/SCID, Charles River, Japan). After about 8–12 weeks, the tumors were extracted from the hind legs and fixed with 4% paraformaldehyde (Sigma) in phosphate buffered solution (PBS), then embedded in paraffin and sectioned for histological analysis by hematoxylin and eosin staining. EBs were grown by floating culture of unattached iPS cell colonies in ESM without β-mercaptethanol, hLIF and hbFGF. After 2 weeks, EBs were cultured in DMEM with 10% FBS for attachment culture. The cells that had spontaneously differentiated from EBs were observed and analyzed by immunofluorescence. To

Table 1
Primer sets used in this study.

Gene	Forward	Reverse	bp
Endogenous POU5F1	GAGAACAATGAGAACCTTCAGGAGA	TTCTGGCGCCGGTTACAGAACCA	60
Endogenous SOX2	CCCCCGGCGGCAACGCA	TCGGCGCCGGGGAGATACAT	51
Endogenous KLF4	GAGCTCTCCCACATGAAGCGA	CGGAATGTACACCGGGTCCAA	51
Endogenous c-MYC	GAGGAGACATGGTGAACCAG	TCGAGGAGAGCAGAGAATCC	49
NANOG	CAGAAGGCCTCAGCACCT	GACTGTTCCAGGCCTGATTGTT	49
REX1	CGAAAACAGCTCGCAGAA	CAGCCTTCAAAGGGACAC	42
GAPDH	TGGACCTGACCTGCCGTCT	GGAAGAGTGGGTGTCGCTGT	49
Exogenous POU5F1	GACGGCATCGCAGCTTGGATACAC	TGAGAGGTCTCCAAGCCACCTT	50
Exogenous SOX2	GACGGCATCGCAGCTTGGATACAC	ATAATCCGGGTGCTCCTTCAT	47
Exogenous KLF4	GACGGCATCGCAGCTTGGATACAC	AATTGGAGAGGATAAAGTCCA	43
Exogenous c-MYC	GACGGCATCGCAGCTTGGATACAC	AGCTCGGTCACCATCTCCAGCT	50
AFP	TGCCAACTCAGTGAGGACAA	TCCAACAGGCCTGAGAAATC	356
Brachyury	ACCCAGTTCATAGCGGTGAC	CAATTGTCATGGGATTGCAG	392
GATA4	GCCTCTACATGAAGCTCCA	GGCTGTTCCAAGAGTCCTGC	401
Pax6	ACAGACACAGCCCTCACAAAC	ATCATAACTCCGCCCATTCACC	159
Cdx2	TCAGCCAGGTCCTCTGAGAA	GCCTGGAATTGCTCTGCC	169
VASA	CCAGAGGGCTGGATATTGAA	TGCAGGAACATCCTGTTGAG	206
β-Actin	TGAAGATCCTCACTGAGCGC	CTCTTCTCCAGGGAGGAGCT	148

examine the differentiation ability of the cells by reverse transcription polymerase chain reaction (RT-PCR), EBs at weeks 1, 2, 3 and 4 of floating culture were collected, respectively.

2.5. Gene expression analysis

Undifferentiated iPS cells and EBs at days 7, 14, 21 and 28 of culture were treated with RNA *later* (Ambion, Austin, TX, USA). RNA was isolated using an RNAqueous Kit (Ambion) according to the manufacturer's protocol. First-strand cDNA was primed via random hexamers and RT-PCR was performed with TaKara Ex Taq, TaKaRa PCR Thermal Cycler Dice Mini and a Thermal Cycler Dice Real Time System (TAKARA BIO INC., Shiga, Japan). The primer sets are shown in Table 1.

2.6. Immunocytochemistry

For immunofluorescence analysis, undifferentiated and differentiated cells were fixed with 4% paraformaldehyde in PBS for 20 min. Following permeabilization with 0.2% Triton X-100 (Sigma) in PBS for 10 min and blocking with 5% FBS in PBS for 30 min, cells were incubated with primary antibodies overnight at 4 °C and visualized by IgG or IgM conjugated with Alexa 488 (A11001, A21042, A11008, A1106, A21212) or 555 (A21428, A21422) (All 1:1000, Invitrogen). The primary antibodies used were as follows: Oct-3 (1:50, Becton Dickinson, 611203), Nanog (1:50, Repro CELL Inc., Tokyo, Japan, RCAB0003P), SSEA1 (sc-21702,), SSEA3 (sc-21703), SSEA4 (sc-21704), TRA-1-60 (sc021705), TRA-1-81 (sc-21706), and TRA-2-54 (sc-21707) (all 1:80, Santa Cruz Biotechnology, Inc. CA, USA) for undifferentiated cells, and Brachyury (1:50, Abcam, Cambridge, UK, ab20680), α-smooth muscle actin (1:100, R&D Systems, Minneapolis, MN, USA, MAB1420), β-tubulin III (1:50, Sigma, T8660) and FOXA2 (1:100, Millipore, AB4125) for differentiated cells. The nuclei were stained with 10 μg/mL Hoechst 33342 (Calbiochem, Darmstadt, Germany) in PBS.

2.7. Karyotyping

Karyotype analyses were performed at the International Council for Laboratory Animal Science Monitoring Center (Kanagawa, Japan).

3. Results

3.1. Generation of iPS cells

To investigate the viability of introducing transgenes into cells from newborn skin and fetal liver (Fig. 1A and B) using retroviral vectors produced from Plat-A cells, we first examined the efficiency of introduction of the GFP gene. The results showed that the percentages of cells expressing GFP among the total cells from the newborn skin and fetal liver samples were 77% and 68%, respectively, as determined by flow cytometry analysis (Fig. 1C and D), demonstrating the effectiveness of infection with retrovirus from Plat-A cells. Indeed, after about four weeks, ES cell-like colonies began to appear among cells from the fetal liver samples into which the four transgenes, POU5F1, SOX2, KLFf4 and c-MYC, had been introduced by retroviral vectors. We obtained 1 and 74 colonies from newborn skin and fetal liver, respectively (Fig. 1E and F). To clarify the characteristics of these colonies, we examined one line from newborn skin (S-1) and five lines from fetal liver (H-1 to H-5). The examined cell lines could be maintained by using the same methods as used for the primate ES cell lines and exhibited a flat colony morphology made up of cells with large nuclei (Fig. 1G and H).

3.2. Characterization of undifferentiated iPS cells

We examined the expression of undifferentiated markers and transgenes, as well as karyotypes, in the iPS cell lines. Immunofluorescence analysis revealed that these cell lines expressed Oct-3, SSEA4, TRA-2-54, TRA-1-60, TRA-1-81 and Nanog, but not SSEA1 and SSEA3 (Fig. 2), which was identical to the expression profile for the cynomolgus monkey ES cell lines. RT-PCR analysis revealed that these cell lines expressed endogenous POU5F1, SOX2, c-MYC, KLF4, Nanog and REX1, but not exogenous POU5F1, SOX2, c-MYC and KLF4, with the exception that exogenous c-MYC was expressed in the H-2 line (Fig. 3). In short, the expressions of the four transgenes introduced by retroviral vectors were almost silenced. Karyotyping analysis revealed that 82% (41/50), 86% (43/50), 78% (39/50) and 82% (41/50) of the S-1 (passage 23), H-1 (passage 28), H-4 (passage 23) and H-5 (passage 26) cell lines examined had a normal chromosome number of 40 and sex chromosomes XX (Fig. 4).

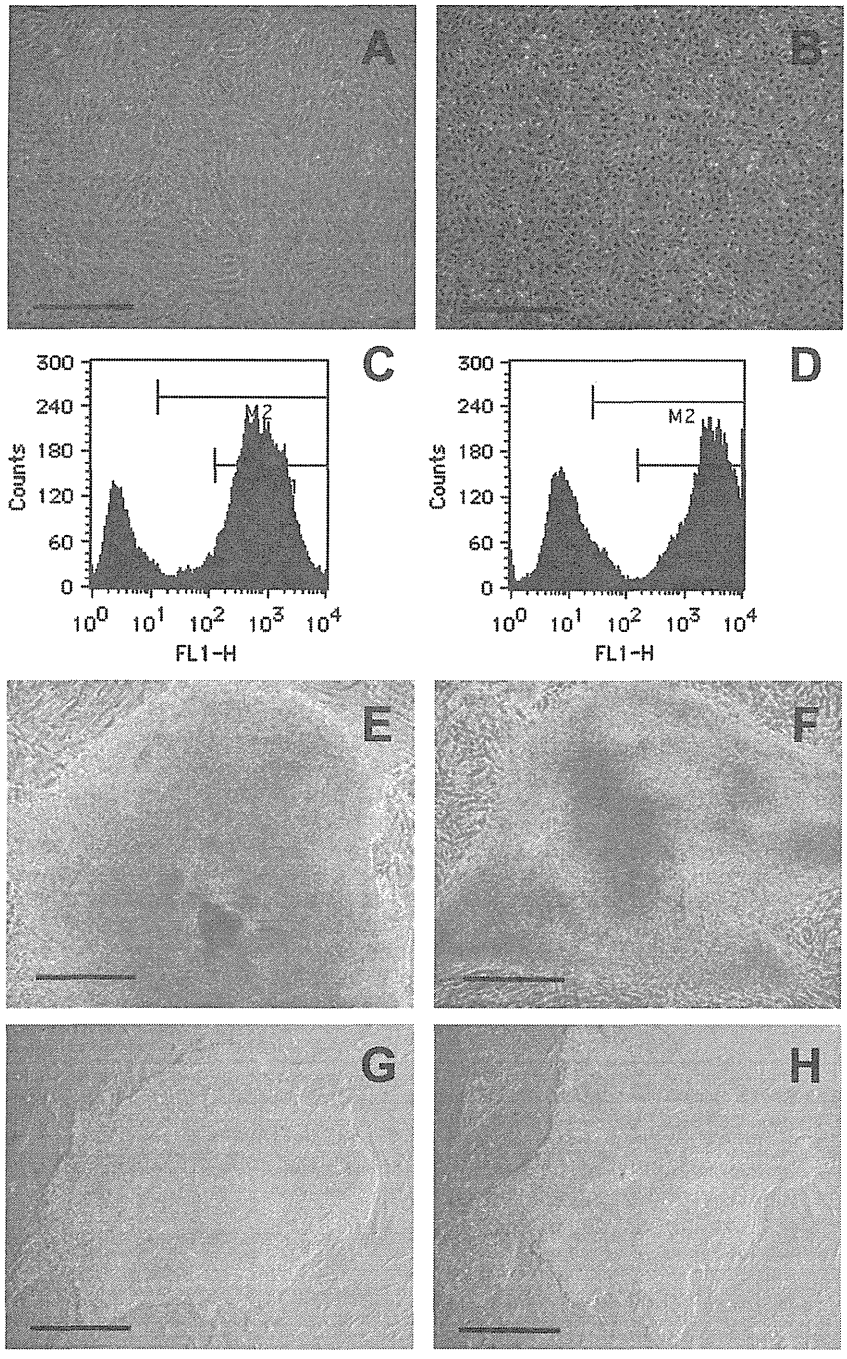

Fig. 1. Generation of iPS cell lines. The cells from newborn skin (A) and fetal liver (B) in cynomolgus monkey were cultured *in vitro*. FACS analysis revealed that, by using retroviral vectors produced from Plat-A cells, the rate of introduction of the GFP gene into both types of somatic cells was relatively high (77% and 68%, respectively) (C,D). By infection of retroviral vectors with POU5F1, SOX2, KLF4 and c-MYC into both types of somatic cells, iPS cell colonies were generated (E,F). The colonies could be maintained using the same method as for primate ES cell lines and showed flat colonies consisting of cells with large nucleoli (G,H). The bar represents 500 μm.

3.3. Characterization of differentiated iPS cells

We examined teratoma formation as *in vivo* differentiation, and EB formation and the expression of differentiated markers as *in vitro* differentiation. We transferred the iPS cell line into two immunodeficient mice. Four of the five transferred iPS cell lines formed, tumors, but not the H-1 line. Histological analysis revealed that the formed tumors were teratomas consisting of ectoderm, endoderm and mesoderm tissues (Fig. 5). After two weeks of the floating culture, most EBs formed solid-type clusters (Fig. 6A). EBs at 2 weeks were transferred to tissue culture dishes and outgrew. EBs spontaneously differentiated into various cell types, such as neuron-like cells, beating myocardial-like cells and pigment cells (Fig. 6B–D). Immunofluorescence analysis revealed the expression of β-tubulin III (ectoderm marker), Foxa2 (endoderm marker), and α-smooth muscle actin and Brachyury (mesoderm markers) in the

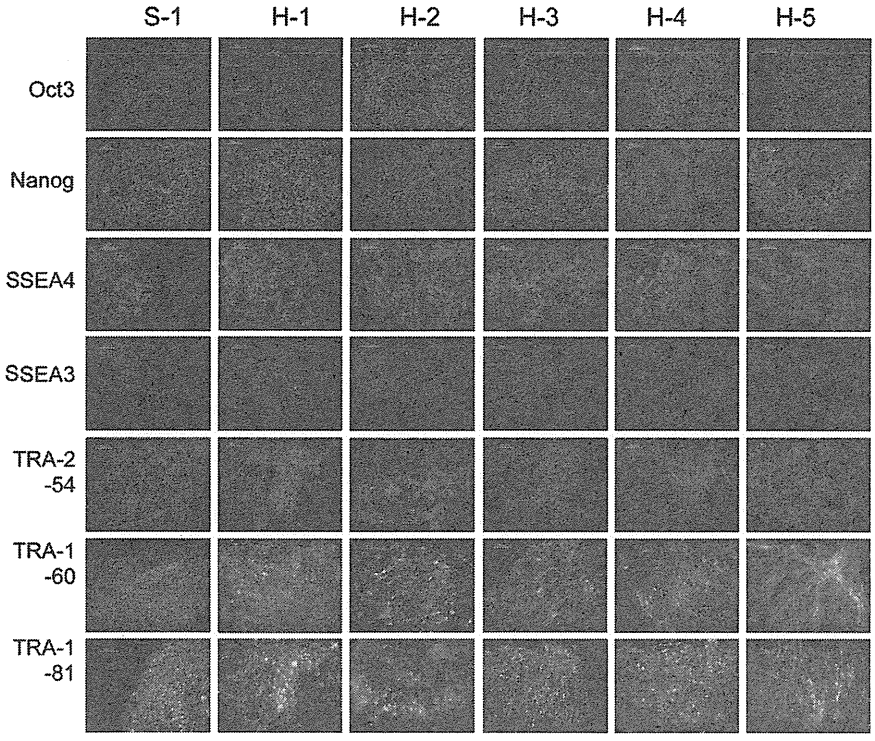

Fig. 2. Immunofluorescence analysis of undifferentiated markers in iPS cells. All cell lines expressed Oct-3, Nanog, SSEA4, TRA-2-54, TRA-1-60 and TRA-1-81, but not SSEA3, which was the same result as in cynomolgus monkey ES cell lines. Nuclei were counterstained with Hoechst 33342.

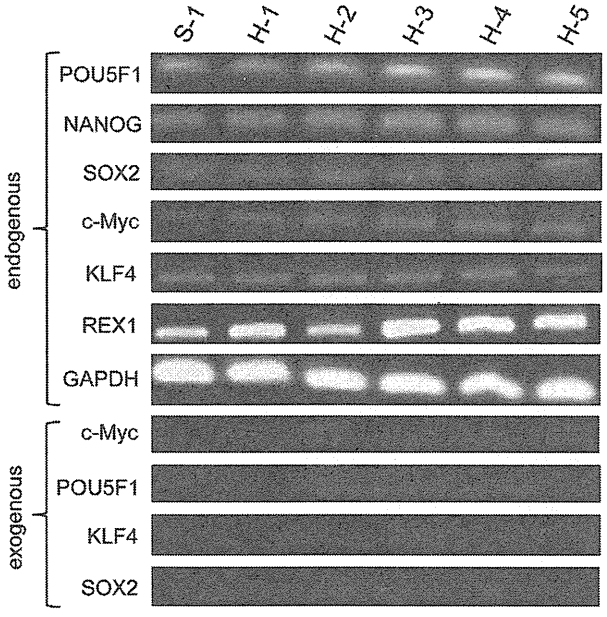

Fig. 3. Gene expression analysis by RT-PCR in iPS cell lines. All cell lines expressed endogenous POU5F1, SOX2, c-MYC, KLF4, Nanog and REX1, but not exogenous POU5F1, SOX2, c-MYC and KLF4, with the exception that exogenous c-MYC was expressed in the H-2 line.

spontaneously differentiated cells from EBs (Fig. 6E–H). In addition, in EBs at days 7, 14, 21 and 28 of culture, we examined the expression of the differentiated markers by RT-PCR. The expression of Brachyury, Pax6 and VASA was detected continuously, and the expression of AFP, GATA4 and CDX2 was detected partially (Fig. 7). In particular, expression of VASA was up-regulated as the *in vitro* culture progressed, and for AFP and CDX2, strong expression was identified in the later stages of the *in vitro* culture.

4. Discussion

We succeeded in establishing iPS cells from cynomolgus monkey somatic cells by using genes taken from the monkeys themselves. The examined iPS cell lines had characteristics similar to other primate ES cell lines. Our study will thus contribute to the development of research resources for a wide range of medical investigations using cynomolgus monkeys. To the best of our knowledge, this is the first report to describe the establishment of iPS cell lines by using cynomolgus monkey genes.

Although ES cells have the potential to make a major contribution to regenerative medicine, until recently, public concerns over the ethics of destroying early human embryos had limited their use. Takahashi and Yamanaka (2006) performed a landmark study to address this problem. They succeeded in directly inducing pluripotent stem cells from somatic cells in mice. By applying this technique, iPS cell lines have been established in humans (Takahashi et al., 2007; Yu et al., 2007), rats (Liao et al., 2009; Li et al., 2009), pigs (Esteban et al., 2009; Wu et al., 2009), rhesus monkeys (Liu et al., 2008), common marmosets (Tomioka et al., 2010), rabbits (Honda et al., 2010) and cynomolgus monkeys (Okahara-Narita et al., 2012). However, the establishment of iPS cell lines using a species' own genes has been achieved only in mice, humans and rhesus monkeys, while in the other species, genes taken from humans or mice were used (Liao et al., 2009; Li et al., 2009; Esteban et al., 2009; Wu et al., 2009; Tomioka et al., 2010; Honda et al., 2010; Okahara-Narita et al., 2012). We here reported on the establishment of iPS cells generated from somatic cells by using genes taken from cynomolgus monkeys.

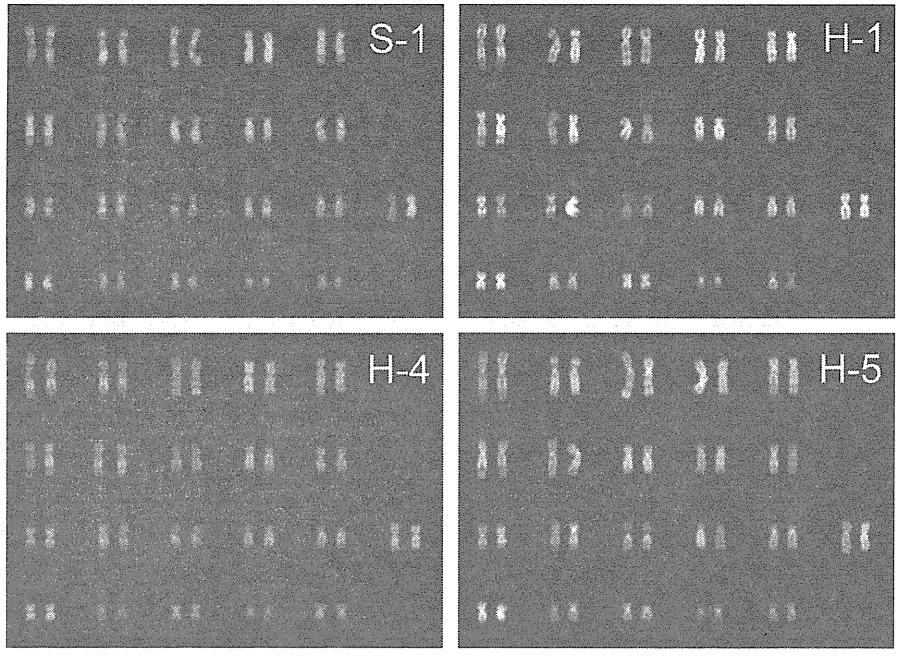

Fig. 4. Karyotyping analysis revealed that 82% (41/50), 86% (43/50), 78% (39/50) and 82% (41/50) of the S-1 (passage 23), H-1 (passage 28), H-4 (passage 23) and H-5 (passage 26) lines examined had a normal chromosome number of 40 and sex chromosomes XX.

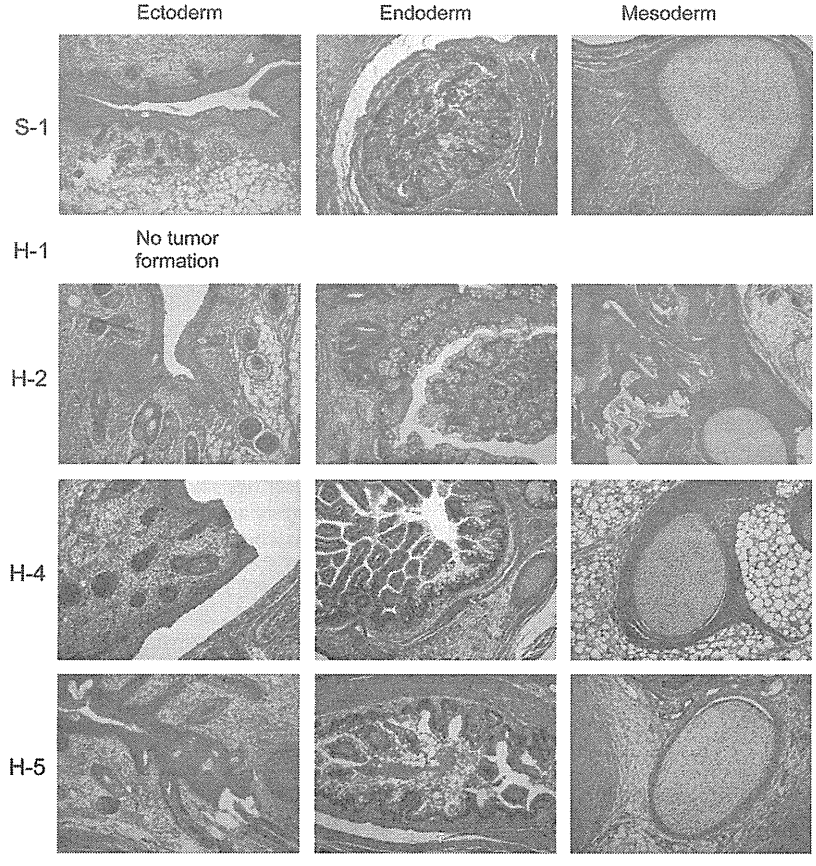

Fig. 5. Histological analysis of teratomas formed from iPS cells. Four of the five iPS cell lines transferred into immunodeficient mice formed tumors, but not the H-1 line. Histological analysis revealed that the formed tumors were teratomas consisting of ectoderm (skin), endoderm (gut) and mesoderm (cartilage and bone) tissues.

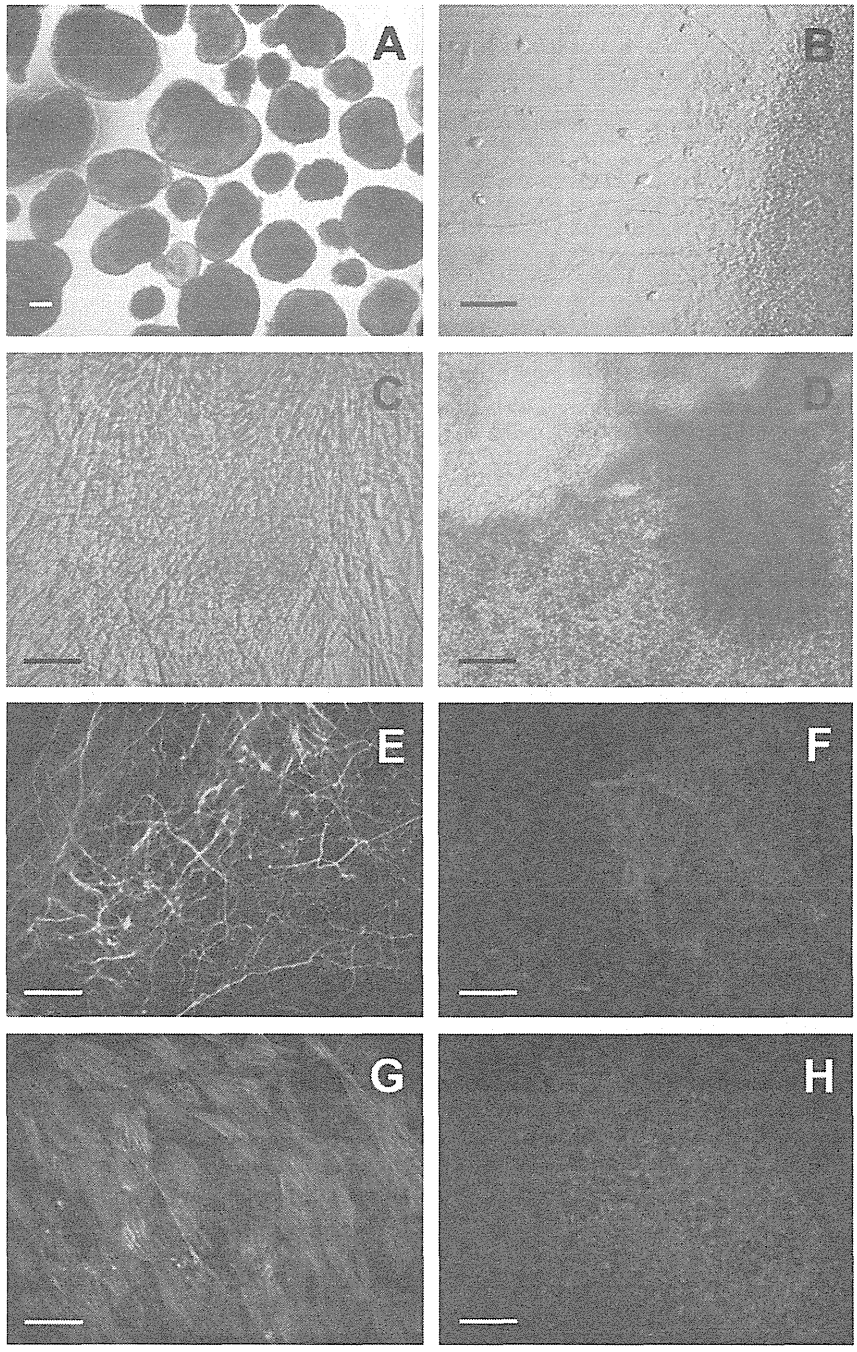

Fig. 6. Analysis of *in vitro* differentiation in iPS cells. Most EBs formed solid-type clusters (A). EBs outgrew on tissue culture dishes and spontaneously differentiated into various cells such as neuron-like cells (B), beating myocardial-like cells (C) and pigment cells (D). Immunofluorescence analysis confirmed the expression of β-tubulin III (E) (ectoderm), Foxa2 (F) (endoderm), and α-smooth muscle (G) and Brachyury (H) (mesoderm) in the cells spontaneously differentiated from EBs. Nuclei were counterstained with Hoechst 33342 (E–H). The bar represents 100 μm.

The cynomolgus monkey iPS cell lines that we established were found to be similar to other primate ES cell lines, including that of cynomolgus monkeys, with respect to characteristics such as morphology, the expression of undifferentiated markers, pluripotency and karyotypic stability. However, the expression of SSEA3, which is one of the ES cell-specific markers, could not be confirmed in the cynomolgus monkey iPS cell lines, although these cell lines could form teratomas consisting of three embryonic germ cells. This feature, the ambiguous expression of SSEA3, was also seen in the cynomolgus monkey ES cell lines (Suemori et al., 2001), while the ES cell lines of other primates, including humans, rhesus monkeys and common marmosets, express SSEA3 (Thomson et al., 1995, 1996, 1998; Sasaki et al., 2005). The results showed that, like primate ES cells, the iPS cell lines established in this study were pluripotent stem cell lines.

We succeeded in establishing iPS cells by using the amphotropic-type retroviral vectors produced from Plat-A cells (Kitamura et al., 2003) for introduction of transgenes into cynomolgus monkey

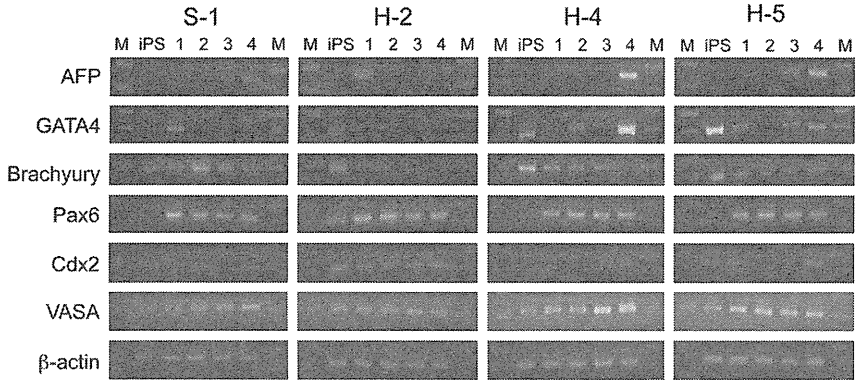

Fig. 7. Gene expression analysis of differentiation markers by RT-PCR in EBs from iPS cells. Expression of differentiation markers was detected by RT-PCR in EBs at days 7, 14, 21 and 28 of culture using four iPS cell lines. Endoderm (AFP, GATA4), mesoderm (Brachyury), ectoderm (Pax6), trophectoderm (CDX2) and germ cell (VASA) markers were analyzed.

somatic cells. Initially, when we examined the introduction of the GFP gene into cells derived from newborn skin and fetal liver, we confirmed the positivity for GFP expression in 77% and 68% of cells, respectively. Because of this highly efficient introduction, we applied the amphotropic retroviral vectors to direct introduction of four transgenes without the introduction of the ecotropic-type retrovirus receptor gene in accordance with the methods of Takahashi et al. (2007) and Okahara-Narita et al. (2012). As a result, we established the iPS cell lines from two kinds of somatic cells. These results showed that the amphotropic-type retroviral vectors could be used to derive pluripotent stem cells, such as mouse and human somatic cells, from cynomolgus monkey somatic cells by introducing the monkey POU5F1, SOX2, KLF4 and c-MYC genes.

The iPS cell lines established in this study expressed the endogenous undifferentiated marker genes POU5F1, NANOG, REX1, SOX2, KLF4 and c-MYC. In contrast, no expression of the transgenes POU5F1, SOX2 and KLF4 was observed in any of the cell lines, while c-MYC expression was observed in a single line. No expression of the four transgenes was observed in five of six cell lines.

In the common marmoset, iPS cell lines have been successfully established by the introduction of five or six genes, but not by the introduction of four genes (Tomioka et al., 2010). However, an important difference between this previously reported study and our present work is that the former used human genes. We and Liu et al. (2008) showed that iPS cell lines could be established using four transgenes from the same species without the introduction of the ecotropic-type retrovirus receptor gene in cynomolgus and rhesus monkeys. The results using two macaque monkeys demonstrate that, by using genes taken from the same species, it may be possible to achieve reprogramming of monkey somatic cells simply and to establish iPS cells suitable for medical research in primates. Furthermore, this may enable detailed analysis of the mechanisms underlying the reprogramming. Elucidating the nature of these mechanisms may in turn contribute to the establishment of an effective method for deriving iPS cells in a completely undifferentiated state without the need to integrate the transgenes into the genome.

We confirmed that, in the established iPS cell lines, expression of VASA, one of the germ cell marker genes (Castrillon et al., 2000; Toyooka et al., 2000), was up-regulated as the *in vitro* culture progressed. This suggested that the iPS cells have the potential to differentiate into germ cells. The differentiation from pluripotent stem cells into germ cells is being studied actively (Clark et al., 2004; Park et al., 2009; Aflatoonian et al., 2009), and the application of this technology to humans is anticipated. The cynomolgus monkeys may predominate in the study of human reproductive medicine because they are annual breeders, unlike rhesus monkeys, which are seasonal breeders.

We succeeded in the establishment of iPS cell lines using four genes taken from the cynomolgus monkeys themselves. When cells differentiated from the iPS cells established with genes from different species are transplanted into monkeys, reactivation of the genes may induce immune responses. Thus an appropriate evaluation based on immune responses may not be possible due to the reactivation of genes from different species. The iPS cell lines that we established will exclude this possibility. In addition, the genes from different species might have unexpected disadvantageous effects. Fortunately, unlike in mice, it is possible to conduct a long-term investigation in monkeys. Therefore, to evaluate the iPS cells established by genes from the same or different species, we plan a long-term investigation of post-transplantation into monkeys in the future.

Author disclosure statement

The authors declare that there are no conflicting financial interests.

Acknowledgments

We thank Professor Toshio Kitamura for the pMXs retroviral vectors and Plat-A cells. This study was supported by grants from the Ministry of Health, Labor and Welfare, and the Ministry of Education, Culture, Sports, Science and Technology of Japan.

References

Aflatoonian, B., Ruban, L., Jones, M., et al., 2009. *In vitro* post-meiotic germ cell development from human embryonic stem cells. Human Reproduction 24, 3150–3159.

Castrillon, D.H., Quade, B.J., Wang, T.Y., et al., 2000. The human VASA gene is specifically expressed in the germ cell lineage. Proceedings of the National Academy of Sciences USA 97, 9585–9590.

Clark, A.T., Bodnar, M.S., Fox, M., et al., 2004. Spontaneous differentiation of germ cells from human embryonic stem cells *in vitro*. Human Molecular Genetics 13, 727–739.

Esteban, M.A., Xu, J., Yang, J., et al., 2009. Generation of induced pluripotent stem cell lines from Tibetan miniature pig. Journal of Biological Chemistry 284, 17634–17640.

Honda, A., Hirose, M., Hatori, M., et al., 2010. Generation of induced pluripotent stem cells in rabbits: potential experimental models for human regenerative medicine. Journal of Biological Chemistry 285, 31362–31369.

Honjo, S., 1985. The Japanese Tsukuba Primate Center for Medical Science (TPC): an outline. Journal of Medical Primatology 14, 75–89.

Kim, K., Doi, A., Wen, B., et al., 2010. Epigenetic memory in induced pluripotent stem cells. Nature 467, 285–290.
Kitamura, T., Koshino, Y., Shibata, F., et al., 2003. Retrovirus-mediated gene transfer and expression cloning: powerful tools in functional genomics. Experimental Hematology 31, 1007–1014.
Li, W., Wei, W., Zhu, S., et al., 2009. Generation of rat and human induced pluripotent stem cells by combining genetic reprogramming and chemical inhibitors. Cell Stem Cell 4, 16–19.
Liao, J., Cui, C., Chen, S., et al., 2009. Generation of induced pluripotent stem cell lines from adult rat cells. Cell Stem Cell 4, 11–15.
Lister, R., Pelizzola, M., Kida, Y.S., et al., 2011. Hotspots of aberrant epigenomic reprogramming in human induced pluripotent stem cells. Nature 471, 68–73.
Liu, H., Zhu, F., Yong, J., et al., 2008. Generation of induced pluripotent stem cells from adult rhesus monkey fibroblasts. Cell Stem Cell 3, 587–590.
Maekawa, M., Yamaguchi, K., Nakamura, T., et al., 2011. Direct reprogramming of somatic cells is promoted by maternal transcription factor Glis1. Nature 474, 225–229.
Nishino, K., Toyoda, M., Yamazaki-Inoue, M., et al., 2011. DNA methylation dynamics in human induced pluripotent stem cells over time. PLoS Genetics 7, e1002085.
Okahara-Narita, J., Umeda, R., Nakamura, S., et al., 2012. Induction of pluripotent stem cells from fetal and adult cynomolgus monkey fibroblasts using four human transcription factors. Primates 53, 205–213.
Okita, K., Ichisaka, T., Yamanaka, S., 2007. Generation of germline-competent induced pluripotent stem cells. Nature 448, 313–317.
Park, T.S., Galic, Z., Conway, A.E., et al., 2009. Derivation of primordial germ cells from human embryonic and induced pluripotent stem cells is significantly improved by coculture with human fetal gonadal cells. Stem Cells 27, 783–795.
Sasaki, E., Hanazawa, K., Kurita, R., et al., 2005. Establishment of novel embryonic stem cell lines derived from the common marmoset (*Callithrix jacchus*). Stem Cells 23, 1304–1313.
Shimozawa, N., Nakamura, S., Takahashi, S., et al., 2010. Characterization of a novel embryonic stem cell line from an ICSI-derived blastocyst in the African green monkey. Reproduction 139, 565–573.
Suemori, H., Tada, T., Torii, R., et al., 2001. Establishment of embryonic stem cell lines from cynomolgus monkey blastocysts produced by IVF or ICSI. Developmental Dynamics 222, 273–279.
Takahashi, K., Yamanaka, S., 2006. Induction of pluripotent stem cells from mouse embryonic and adult fibroblast cultures by defined factors. Cell 126, 663–676.
Takahashi, K., Tanabe, K., Ohnuki, M., et al., 2007. Induction of pluripotent stem cells from adult human fibroblasts by defined factors. Cell 131, 861–872.
Thomson, J.A., Kalishman, J., Golos, T.G., et al., 1995. Isolation of a primate embryonic stem cell line. Proceedings of the National Academy of Sciences USA 92, 7844–7848.
Thomson, J.A., Kalishman, J., Golos, T.G., et al., 1996. Pluripotent cell lines derived from common marmoset (*Callithrix jacchus*) blastocysts. Biology of Reproduction 55, 254–259.
Thomson, J.A., Itskovitz-Eldor, J., Shapiro, S.S., et al., 1998. Embryonic stem cell lines derived from human blastocysts. Science 282, 1145–1147.
Tomioka, I., Maeda, T., Shimada, H., et al., 2010. Generating induced pluripotent stem cells from common marmoset (*Callithrix jacchus*) fetal liver cells using defined factors, including Lin28. Genes to Cells 15, 959–969.
Toyooka, Y., Tsunekawa, N., Takahashi, Y., et al., 2000. Expression and intracellular localization of mouse VASA-homologue protein during germ cell development. Mechanisms of Development 93, 139–149.
Tsuchida, J., Yoshida, T., Sankai, T., et al., 2008. Maternal behavior of laboratory-born, individually reared long-tailed macaques (*Macaca fascicularis*). Journal of American Association Laboratory Animal Science 47, 29–34.
Wu, Z., Chen, J., Ren, J., et al., 2009. Generation of pig induced pluripotent stem cells with a drug-inducible system. Journal of Molecular Cell Biology 1, 46–54.
Yasutomi, Y., 2010. Establishment of specific pathogen-free macaque colonies in Tsukuba Primate Research Center of Japan for AIDS research. Vaccine 28 (Suppl. 2), B75–B77.
Yu, J., Vodyanik, M.A., Smuga-Otto, K., et al., 2007. Induced pluripotent stem cell lines derived from human somatic cells. Science 318, 1917–1920.

Cardiovasc Drugs Ther (2013) 27:413–424
DOI 10.1007/s10557-013-6464-y

ORIGINAL ARTICLE

Pitavastatin Regulates Helper T-Cell Differentiation and Ameliorates Autoimmune Myocarditis in Mice

Kazuko Tajiri · Nobutake Shimojo · Satoshi Sakai · Tomoko Machino-Ohtsuka · Kyoko Imanaka-Yoshida · Michiaki Hiroe · Yusuke Tsujimura · Taizo Kimura · Akira Sato · Yasuhiro Yasutomi · Kazutaka Aonuma

Published online: 31 May 2013

Abstract
Purpose Experimental autoimmune myocarditis (EAM) is a mouse model of inflammatory cardiomyopathy, and the involvement of T helper (Th) 1 and Th17 cytokines has been demonstrated. Accumulated evidence has shown that statins have anti-inflammatory and immunomodulatory effects; however, the mechanism has not been fully elucidated. This study was designed to test the hypothesis that pitavastatin affects T cell-mediated autoimmunity through inhibiting Th1 and Th17 responses and reduces the severity of EAM in mice.
Methods The EAM model was established in BALB/c mice by immunization with murine α-myosin heavy chain. Mice were fed pitavastatin (5 mg/kg) or vehicle once daily for 3 weeks from day 0 to day 21 after immunization.
Results Pitavastatin reduced the pathophysiological severity of the myocarditis. Pitavastatin treatment inhibited the phosphorylation of signal transducer and activator of transcription (STAT)3 and STAT4, which have key roles in the Th1 and Th17 lineage commitment, respectively, in the heart, and suppressed production of Th1 cytokine interferon-γ and Th17 cytokine interleukin-17 from autoreactive $CD4^+$ T cells. In in vitro T-cell differentiation experiments, pitavastatin-treated T cells failed to differentiate into Th1 and Th17 cells through inhibiting the transcription of T-box expressed in T-cells (T-bet) and RAR-related orphan receptor γt (RORγT) which have critical roles in the development of Th1 and Th17 cells, respectively, and this failure was rescued by adding mevalonate.
Conclusions Pitavastatin inhibits Th1 and Th17 responses and ameliorates EAM. These results suggest that statins may be a promising novel therapeutic strategy for the clinical treatment of myocarditis and inflammatory cardiomyopathy.

Keywords Autoimmune myocarditis · Statin · Helper T cells · Inflammation

Electronic supplementary material The online version of this article (doi:10.1007/s10557-013-6464-y) contains supplementary material, which is available to authorized users.

K. Tajiri (✉) · N. Shimojo · S. Sakai · T. Machino-Ohtsuka · T. Kimura · A. Sato · K. Aonuma
Cardiovascular Division, Faculty of Medicine, University of Tsukuba, 1-1-1 Tennodai,
Tsukuba, Ibaraki 305-8575, Japan
e-mail: ktajiri@md.tsukuba.ac.jp

K. Tajiri · T. Machino-Ohtsuka · Y. Tsujimura · Y. Yasutomi
Laboratory of Immunoregulation and Vaccine Research, Tsukuba Primate Research Center, National Institute of Biomedical Innovation, Tsukuba, Ibaraki, Japan

K. Imanaka-Yoshida
Department of Pathology and Matrix Biology, Mie University Graduate School of Medicine, Tsu, Mie, Japan

K. Imanaka-Yoshida
Mie University Matrix Biology Research Center, Mie University Graduate School of Medicine, Tsu, Mie, Japan

M. Hiroe
Department of Cardiology, National Center for Global Health and Medicine, Shinjuku, Tokyo, Japan

Y. Yasutomi
Division of Immunoregulation, Department of Molecular and Experimental Medicine, Mie University Graduate School of Medicine, Tsu, Mie, Japan

Introduction

Dilated cardiomyopathy (DCM) is a potentially lethal disorder of various etiologies for which no treatment is currently satisfactory [1]. Many patients show heart-specific autoantibodies [2, 3], and immunosuppressive therapy can improve their cardiac function [4]. These observations suggest that

autoimmunity plays an important role in myocarditis as well as contributes to the progression to DCM and heart failure [5]. Animal models have greatly advanced our knowledge of the pathogenesis of myocarditis and inflammatory cardiomyopathy. Experimental autoimmune myocarditis (EAM) induced by cardiac myosin immunization is a model of postinfectious myocarditis and DCM [6–8]. EAM represents a $CD4^+$ T cell-mediated disease [6, 9, 10] and has been considered to be associated with both interferon (IFN)-γ producing T helper (Th)1 cells and interleukin (IL)-17 producing Th17 cells [10].

Statins are orally administered competitive inhibitors of 3-hydroxy-3-methylglutaryl coenzyme A (HMG-CoA) reductase, an enzyme that catalyzes the conversion of HMG-CoA to mevalonate. As effective cholesterol-lowering agents, statins have been extensively used for prevention of cardiovascular disease [11]. In the past few years, accumulated evidence from animal experiments and clinical studies has shown that statins have anti-inflammatory and immunomodulatory effects. The effects of statins on the immune system are pleiotropic and include inhibition of T-cell activation, proliferation, and migration [12–14]. Reportedly, atorvastatin was able to promote shifting of the T-cell response from a pro-inflammatory Th1 to an anti-inflammatory Th2 profile in experimental autoimmune encephalomyelitis (EAE), an animal model of multiple sclerosis mediated by Th1 cells in the central nervous system [15, 16]. Furthermore, simvastatin was able to inhibit IL-17 secretion which plays a critical role in the development of autoimmune diseases, in $CD4^+$ T cells derived from relapsing remitting multiple sclerosis patients [17]. Although this evidence suggests that statins can inhibit Th1 and Th17 inflammatory responses in autoimmune diseases, the mechanism has not been fully elucidated.

Based on these effects of statins, this study was designed to test the hypothesis that pitavastatin affects T cell-mediated autoimmunity through inhibiting Th1 and Th17 responses and reduces the severity of EAM in mice.

Materials and Methods

Study Approval

All animal experiments were approved by the Institutional Animal Experiment Committee of the University of Tsukuba.

Mice

BALB/c mice and CB17.SCID mice were purchased from CLEA Japan. We used 5- to 7-week-old male mice.

Immunization Protocols

The mice were immunized with 100 μg of murine cardiac α-myosin heavy chain (MyHC-α) peptide (MyHC-$\alpha_{614-629}$ [Ac-RSLKLMATLFSTYASADR-OH]; Toray Research Center) emulsified 1:1 in phosphate buffered saline (PBS)/complete Freund's adjuvant (CFA) (1 mg/ml; H37Ra; Sigma-Aldrich) on days 0 and 7 as described previously [10, 18].

In Vivo Pitavastatin Treatment

Pitavastatin was obtained from the Kowa Company and diluted with distilled water before use. Mice were fed pitavastatin (5 mg/kg) or vehicle once daily by gavage feeding for 3 weeks from day 0 to day 21 after immunization. In some experiments, EAM mice were treated with 0.05, 0.5 or 5 mg/kg of pitavastatin.

Histopathologic Examination

Myocarditis severity was scored on hematoxylin and eosin (H&E)–stained sections using grades from 0 to 4: 0, no inflammation; 1, less than 25 % of the heart section involved; 2, 25 to 50 %; 3, 50 to 75 %; and 4, more than 75 % as described previously [10, 18]. Two independent researchers scored the slides separately in a blinded manner.

Flow Cytometric Analyses and Intracellular Cytokine Staining

Heart inflammatory cells were isolated and processed as previously described [19, 20]. For the flow cytometric analysis of the surface markers and cytoplasmic cytokines, the cells were stained with directly conjugated fluorescence antibodies and analyzed with a FACSCalibur instrument (BD Biosciences). For the analysis of the intracellular cytokine production, the cells were stimulated with 50 ng/ml of phorbol 12-myristate 13-acetate (PMA), 750 ng/ml of ionomycin (Sigma-Aldrich) and 10 μg/ml of brefeldin A (eBioscience) for 5 h. Fluorochrome-conjugated, mouse-specific monoclonal antibodies purchased from eBioscience, included CD4, forkhead box P3 (Foxp3), IFN-γ, IL-17A, T-box expressed in T-cells (T-bet) and RAR-related orphan receptor γt (RORγT).

Cytokine ELISA

For the analysis of the cytokines and chemokines in the heart, the hearts were homogenized in media containing 2.5 % fetal bovine serum. The supernatants were collected after centrifugation and stored at −80 °C. The concentrations of cytokines and chemokines in the heart homogenates and

culture supernatants were measured with Quantikine ELISA kits (R&D Systems).

$CD4^+$ T-Cell Isolation

We used magnetic-activated cell sorting kits for the cell isolation ($CD4^+CD62L^+$ T Cell Isolation Kit II for naïve $CD4^+$ T-cell isolation and $CD4^+$ T Cell Isolation Kit II for $CD4^+$ T cell isolation, Miltenyi Biotec).

Peripheral Blood Mononuclear Cell (PBMC) Isolation

PBMCs were isolated as previously described [21]. Briefly, blood samples were diluted with PBS and the plasma was removed by centrifugation. To remove the red blood cells, the samples were incubated with ACK lysing buffer (Lonza).

Proliferative Responses of T Cells

The MyHC-α-specific T-cell proliferation was assessed as previously described [10, 22]. Briefly, the mice were immunized as described above, and the $CD4^+$ T cells were collected on day 14. The cells were cultured with 5 μg/ml of MyHC-α in the presence of antigen-presenting cells (APCs), and irradiated splenocytes, for 72 h and pulsed with 0.5 μCi of [^{3}H]-thymidine for 8 h before being measured with a beta counter.

Western Blot Analysis

Total lysates from $CD4^+$ T cells were immunoblotted and probed with primary Abs. The phosphorylated (p)-signal transducer and activator of transcription (STAT)3 was purchased from Cell Signaling. STAT3, STAT4, STAT6, p-STAT4 and p-STAT6 were purchased from Santa Cruz Biotechnologies. Horseradish peroxidase-conjugated secondary antibodies (Abs) (Cell Signaling) were used to identify the binding sites of the primary antibody.

Serum Troponin Determinations

Blood was collected from the mice at the time of sacrifice, and the serum levels of cardiac troponin I (TnI) were measured with an ELISA kit (mouse cardiac Tn-I, ultra sensitive; Life Diagnostics).

Reagents and Inhibitors

For the in vitro assay, reagents and inhibitors were used in the following concentrations: pitavastatin 1 μM, mevalonate 1 mM (Sigma), farnesyltransferase inhibitor (FTI-277) 20 μM (Sigma-Aldrich), geranylgeranyltransferase inhibitor (GGTI-298) 20 μM (Sigma-Aldrich), anti-CD3 1 μg/ml (R&D Systems), anti-CD28 1 μg/ml (Acris Antimodies), farnesylpyrophosphate (farnesyl-PP) 20 μM (Sigma-Aldrich) and geranylgeranylpyrophosphate (geranylgeranyl-PP) 20 μM (Sigma-Aldrich).

In Vitro Th Differentiation

Purified naïve $CD4^+CD62L^+$ T cells were treated for 24 h with pitavastatin, mevalonate, FTI-277, GGTI-298, or vehicle; then they were stimulated with anti-CD3 and anti-CD28 under Th1- or Th17- polarizing conditions for 48 h. Th1 condition: IL-12 (10 ng/ml) and anti-IL-4 antibody (10 μg/ml). Th17 condition: transforming growth factor (TGF)-β (10 ng/ml), IL-6 (20 ng/ml), IL-23 (20 ng/ml), anti–IL-4 (10 μg/ml), anti–IL-12 (10 μg/ml) and anti–IFN-γ (10 μg/ml). The cytokines and antibodies were obtained from R&D systems except for the TGF-β (BioLegend).

Adoptive T-Cell Transfer

$CD4^+$ T cells were collected from EAM mice and cultured with 5 μg/ml MyHC-α in the presence of irradiated splenocytes for 48 h. In some experiments, cells were cultured in the presence or absence of 1 μM of pitavastatin. 5×10^6 $CD4^+$ T cells were injected intraperitoneally into severe combined immunodeficiency (SCID) mice. The mice were killed 10 days after the transfer.

Quantitative Real-Time Reverse Transcription Polymerase Chain Reaction (QRT-PCR)

The total RNA was prepared using TRIzol reagent (Invitrogen) according to the manufacturer's instructions. The cDNA was synthesized from 1 μg of the total RNA by reverse transcriptase (Takara). QRT-PCR analysis was performed with LightCycler (Roche Diagnostics). The oligonucleotides used for the PCR amplification of the cytokines and receptors were the following: *Tbx21* forward, TCAACCAGCACCAGACAGAG; *Tbx21* reverse, AAACATCCTGTAATGGCTTGTG; *Rorc* forward, CCCTGGTTCTCATCAATGC; *Rorc* reverse, TCCAAATTGTATTGCAGATGTTC; *Socs3* forward, ATTTCGCTTCGGGACTAGC; *Socs3* reverse, AACTTGCTGTGGGTGACCAT; *Hprt* forward, TCCTCCTCAGACCGCTTTT; and *Hprt* reverse CCTGGTTCATCATCGCTAATC. The data were normalized by the level of the *Hprt* expression in each sample.

Statistical Analysis

Statistical analyses were performed using the two-tailed *t* test or Mann–Whitney *U* test, for experiments comparing two groups. For multiple comparisons, one-way analysis of

variance with Dunnett post-hoc test was used. P values< 0.05 were considered statistically significant.

Results

Pitavastatin Inhibits the Development of EAM

First, we sought to determine the in vivo effects of pitavastatin on EAM. BALB/c mice were fed pitavastatin (5 mg/kg) or vehicle (control) once daily by gavage feeding, starting from the beginning of the MyHC-α immunization and lasting to the end of the experiment. As shown in Fig. 1a, vehicle-treated mice (control) developed severe myocarditis with inflammatory infiltrates. In contrast, pitavastatin treatment of mice resulted in a significant reduction in the inflammatory infiltrates in the heart. Pitavastatin-treated mice had a significantly lower myocarditis severity score than did the control mice (Fig. 1b). The heart-to-body weight ratio in the pitavastatin-treated mice was significantly decreased compared to that in the control mice (Fig. 1c), as were the levels of the circulating cardiac TnI, a clinical marker of myocyte damage (Fig. 1d). We also examined whether pitavastatin treatment had an effect on the cytokine and chemokine milieu in the heart. On day 21 after the MyHC-α immunization, the heart homogenates from pitavastatin-treated mice had significantly decreased amounts of proinflammatory cytokines, including IL-1β and IL-6, and chemokines, including chemokine (C-C motif) ligand (CCL)2, CCL3, CCL5, CCL17, CCL20 and chemokine (C-X-C motif) ligand (CXCL)10 (Fig. 1e). Thus, pitavastatin ameliorated EAM development, which corresponded to the abrogation of the proinflammatory cytokines and chemokines in the heart.

Pitavastatin Induced SOCS3 Expression and Suppressed STAT3 and STAT4 Phosphorylation

EAM is a $CD4^+$ T cell-mediated disease [6, 20] and both Th1 and Th17 cells are linked to the promotion of EAM. Activated STAT4 has a key role in Th1 lineage commitment and STAT3 does so for Th17 [23–25]. Conversely, STAT6 is required for Th2-dependent lineage commitment [23]. Therefore, we examined whether pitavastatin treatment suppressed the formation of activated STAT3 and STAT4 or induced activation of STAT6. In vivo pitavastatin treatment inhibited STAT3 and STAT4 phosphorylation and promoted STAT6 phosphorylation in a dose-dependent manner (Fig. 2a). Accordingly, heart-infiltrating and circulating IFN-γ- and IL-17-producing $CD4^+$ T cells were reduced in pitavastatin-treated mice

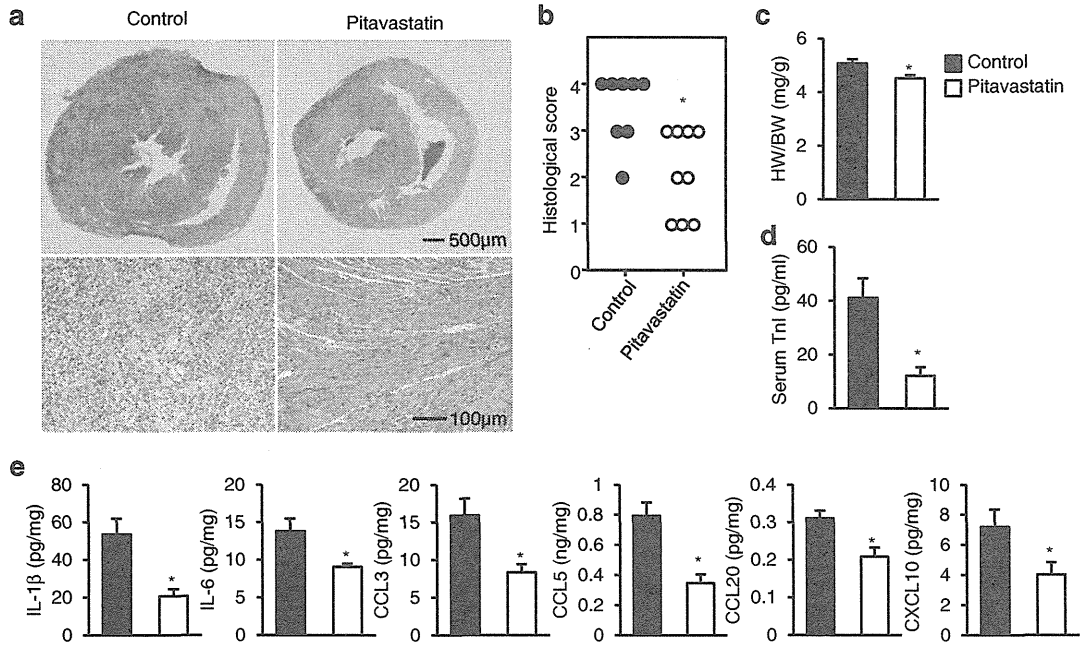

Fig. 1 Pitavastatin ameliorates the EAM development. BALB/c mice were immunized twice, on days 0 and 7, with 100 μg of cardiac myosin epitope peptide (MyHC-α) and treated with pitavastatin (5 mg/kg) or vehicle (control) for 3 weeks from day 0 to day 21 after immunization. **a** Representative H&E-stained sections of the hearts. Scale bars, 500 or 100 μm. **b** Myocarditis severity in heart sections (n=8–9 per group). **c** Heart-to-body weight ratios of control and pitavastatin-treated mice (n=5 per group). **d** Circulating troponin I (TnI) concentration (n=5 per group). **e** Production of cytokines and chemokines in the hearts. Myocardial tissues of vehicle- and pitavastatin-treated EAM mice were homogenated and processed by ELISA to detect the cytokines and chemokines on day 21. The *bar graphs* show the group means ± SEM of 8 mice per group. The results of one of two representative experiments are shown. Data are expressed as the mean ± SEM. *P<0.05 vs. control

(Fig. 2b and c). Foxp3$^+$ regulatory T cells (Tregs) are known to play a crucial role in preventing autoimmune disorders and actively controlling autoimmune responses [26, 27]. Therefore, we examined the effect of pitavastatin on Tregs in EAM. There were no differences in the frequencies of Foxp3$^+$ Tregs in the heart and PBMCs (Fig. 2d). The MyHC-α-specific proliferative responses of CD4$^+$ T cells were reduced by pitavastatin treatment in a dose-dependent manner (Fig. 2e). We also found that the MyHC-α-specific production of IFN-γ and IL-17 was reduced in supernatants of CD4$^+$ T cells from pitavastatin-treated mice (Fig. 2f). We could not detect any Th2 cytokine IL-4 production from the heart and splenic CD4$^+$ T cells in either the control or pitavastatin-treated mice.

STAT activation is partially regulated by the expression of inhibitory SOCS proteins. We thus assessed the expression of SOCS3 and STAT phosphorylation in pitavastatin-treated T cells. Vehicle-treated T cells downregulated the *Socs3* mRNA expression after activation, whereas pitavastatin-treated T cells retained a higher expression (Fig. 2g). Mevalonate reversed the effects of pitavastatin on the *Socs3* expression (Fig. 2g). In contrast, pitavastatin treatment inhibited STAT3 and STAT4 phosphorylation, and mevalonate reversed the inhibitory effects of pitavastatin on the STAT activation (Fig. 2h). Such observations demonstrate that pitavastatin upregulates the

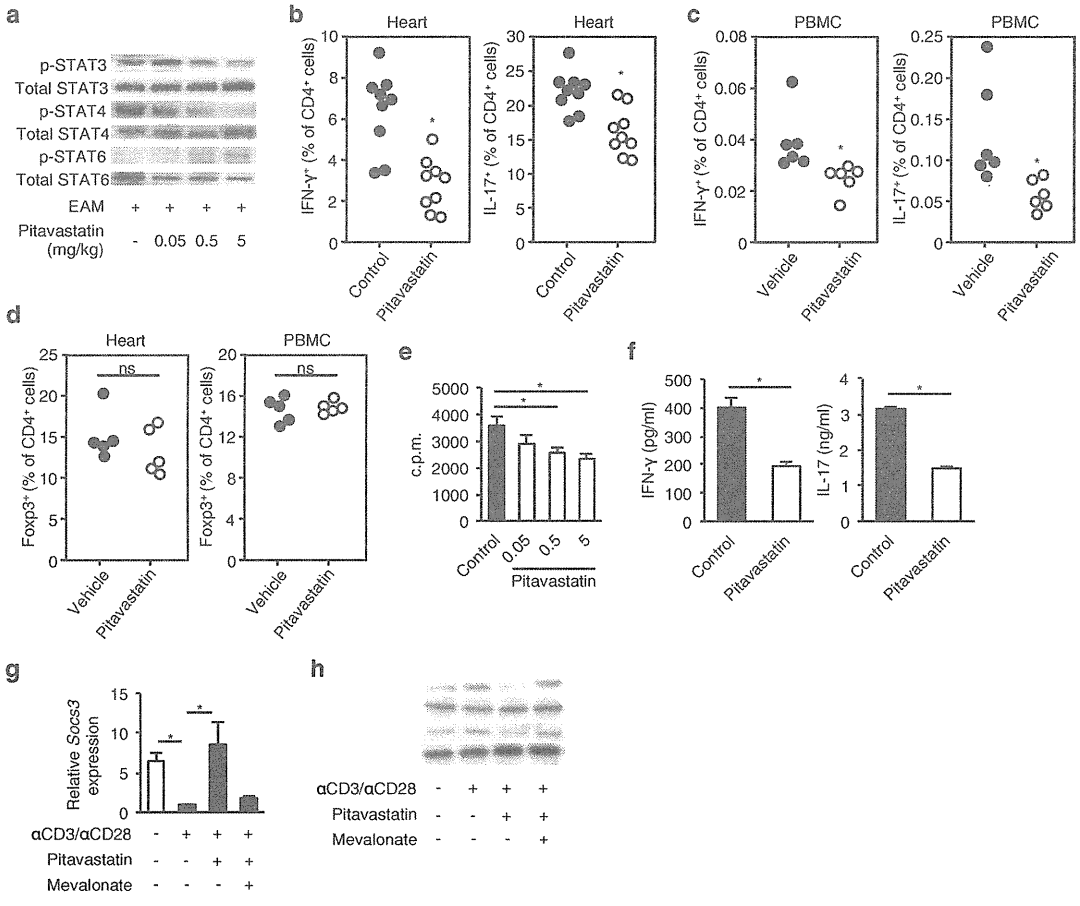

Fig. 2 Pitavastatin increases the SOCS3 expression and suppresses phosphorylation of STAT3 and STAT4. **a** STATs activation in CD4$^+$ T cells. CD4$^+$ T cells were isolated from the heart of vehicle-treated EAM mice, and EAM mice treated with 0.05, 0.5 or 5 mg/kg of pitavastatin. The phosphorylated and total STAT3, STAT4 and STAT6 proteins were detected by Western blot analysis. **b–d** Flow cytometry analysis of IFN-γ- or IL-17-producing CD4$^+$ T cells or Fop3+ Tregs in the hearts and PBMC from 5 mg/kg of pitavastatin- or vehicle-treated mice (n=5–9 per group). **e** CD4$^+$ T cells were isolated from EAM mice treated with pitavastatin or vehicle on day 14 and restimulated with MyHC-α in the presence of APCs (irradiated splenocytes) for 72 h. Proliferation was assessed by a measurement of the [^{3}H]-thymidine incorporation. **f** The MyHC-α-specific IFN-γ and IL-17 production in the culture supernatant of CD4$^+$ T cells. CD4$^+$ T cells were isolated from 5 mg/kg of pitavastatin- or vehicle-treated EAM mice and cultured with 5 μg/ml of MyHC-α in the presence of APCs for 2d. **g** The *Socs3* mRNA expression in CD4$^+$ T cells treated for 18 h with the indicated agents and then stimulated with anti-CD3 and anti-CD28 for 6 h. The data were normalized for the basal gene expression in anti CD3- and anti CD28-treated cells. **h** STATs activation in CD4$^+$ T cells. CD4$^+$ T cells were treated as described in (**g**), and the phosphorylated and total STAT3 and STAT4 proteins were detected by Western blot analysis. Data are expressed as the mean ± SEM from triplicate culture wells. The results of one of two representative experiments are shown. *P<0.05